5-4-2020

Hemoglobin and the Host Pathogen Interactions in Streptococcus pneumoniae: a New Paradigm

Fahmina Akhter
Georgia State University

HEMOGLOBIN AND THE HOST PATHOGEN INTERACTIONS IN *STREPTOCOCCUS PNEUMONIAE*: A NEW PARADIGM

by

FAHMINA AKHTER

Under the Direction of Zehava Eichenbaum, PhD

ABSTRACT

Streptococcus pneumoniae is a principal human pathogen that colonizes the human nasopharynx and causes a variety of diseases ranging from common infections to life-threatening conditions such as pneumonia, meningitis, and sepsis. During infection, free iron is not available, and thus, invading microbes, such as *S. pneumoniae*, compete with the host for the metal. The heme-iron bound to hemoglobin is the most abounded form of iron in the human body. *S. pneumoniae* can obtain iron from hemoglobin, but the bacterial mechanisms involved in this process are only partially described. This dissertation investigated the role of hemoglobin in pneumococcal physiology and virulence. The studies discovered that hemoglobin promotes vigorous *S. pneumoniae* growth. The pneumococcal growth response is hemoglobin dependent,

conserved among pneumococcal serotypes, and not seen with free heme or iron. Hemoglobin also induces an extensive transcriptome remodeling, effecting virulence factors and metabolism, and in particular genes that facilitate the use of host glycoconjugates as a sugar source. The second significant finding of this study is the discovery that hemoglobin promotes robust and early pneumococcal biofilms. The biofilm response is hemoglobin specific, and free iron, heme, or other heme sources such as myoglobin and serum do not induce the response. The addition of human blood also triggers biofilms but required the pneumococcal hemolysin, Ply. *S. pneumoniae* cells shifting from planktonic growth to biofilms in the presence of hemoglobin exhibit a significant transcriptome shift that includes heme uptake and regulatory systems. The biofilm response to hemoglobin involves the CiaRH two-component system, and the Competence Stimulating Peptide, CSP-1. The data shows that CSP-1 functions in a new mechanism that is independent of its cognate two-component system ComDE. In summary, this dissertation describes a novel role for the host hemoglobin in pneumococcal physiology and pathogenesis. It discusses how these findings advance the current understanding of *S. pneumoniae* interactions with its obligate human host.

INDEX WORDS: *Streptococcus pneumoniae*, Hemoglobin, Transcriptome, Host glycoconjugates, Nasopharyngeal colonization, Biofilm, CSP, CiaRH.

HEMOGLOBIN AND THE HOST PATHOGEN INTERACTIONS IN *STREPTOCOCCUS PNEUMONIAE*: A NEW PARADIGM

by

FAHMINA AKHTER

A Dissertation Submitted in Partial Fulfillment of the Requirements for the Degree of

Doctor of Philosophy

in the College of Arts and Sciences

Georgia State University

2020

HEMOGLOBIN AND THE HOST PATHOGEN INTERACTIONS IN *STREPTOCOCCUS PNEUMONIAE*: A NEW PARADIGM

by

FAHMINA AKHTER

Committee Chair: Zehava Eichenbaum

Committee: Kuk-Jeong Chin

Eric Gilbert

Jorge Vidal

Electronic Version Approved:

Office of Graduate Services

College of Arts and Sciences

Georgia State University

May 2020

DEDICATION

TO MY FAMILY

My parents, my husband, and my sons without whom this doctoral journey would not be possible.

ACKNOWLEDGEMENTS

First, I would like to express my heartfelt gratitude to my supervisor Dr. Zehava Eichenbaum for her guidance, support, and encouragement for my dissertation research. Thank you for the opportunity to work under your leadership and for the inspiration you provided throughout my doctoral program. I highly appreciate your mentorship that allowed me to think scientifically. My sincere appreciation to Dr. Jorge Vidal for his continuous advice and support in my dissertation research. Thank you for providing me the strains and allowing me to work in your lab during my doctoral program. I would like to thank my other committee members, Dr. Eric Gilbert and Dr. Kuk-Jeong Chin, for their guidance and advice. I would like to thank my lab members Edroyal Womack, Kristin Vanmourik Lyles, Nilanjana Chatterjee, for their support. It was a pleasure working with these people who made my doctoral journey in the lab enjoyable. Finally, I can’t express enough gratitude in words to my parents and my husband. Without their constant support, dedication, and unconditional love, I would not be able to pursue my doctoral journey. My parents, my husband, and my sons are the true inspiration in my life. Above all, I am grateful to Almighty Allah for blessing me good health, wisdom, and strength to complete this prestigious part of my life.

TABLE OF CONTENTS

LIST OF TABLES

LIST OF FIGURES

1 GENERAL INTRODUCTION

The purpose of this dissertation is to promote the understanding of the physiology and virulence of the human pathogen *Streptococcus pneumoniae* (Spn). Experiments were centered on heme uptake and pneumococcal adaptation to the host environment. This background section will provide a brief overview of the area of pneumococcal pathogenesis and biofilm formation.

1.1 *Streptococcus pneumoniae* disease burden and vaccine

Spn is an obligate human pathogen that can be carried asymptomatically in the upper respiratory tract [1]. Children are more common carriers of Spn than adults (20–50% and 5–20%, respectively) depending on the sociodemographic status of the countries [2-4]. In some cases, the pathogen migrates to lower airway or other anatomic sites and causes severe infections such as otitis media, pneumonia, meningitis, and sepsis [5, 6]. Spn is the leading cause of bacterial pneumonia, contributing to ~15 million annual cases worldwide and 800,000 deaths in children (<5 years of age) [7, 8]. Pneumococcal pneumonia also increases the risk for the development of cardiac diseases and heart failure [9, 10]. Hosts with under-developed or weak immune systems such as infants, children under five years of age, elderly over 60-65 years of age, or with underlying conditions are the most affected by Spn infections [5, 6, 11]. In addition, Spn coinfections with a viral respiratory pathogen, such as Influenza A or the respiratory syncytial virus, worsen the disease severity and mortality rates [12, 13]. A multivalent vaccine to combat pneumococcal infections is available. But the vaccination program did not cover all the pneumococcal serotypes and increased the prevalence of vaccine-escape serotypes. Hence, Spn remains a global threat [14].

1.2 Spn virulence

Spn undergoes dynamic interactions with host cells employing a magnitude of virulence factors from its initial establishment in the upper respiratory tract and through its spread within the body [1, 15, 16]. The section below elaborates only on the virulence determinants that are important for the experiments describe in this dissertation.

Nasopharyngeal colonization is critical for Spn virulence since it facilitates the pathogen establishments within the host. Spn colonization requires bacterial factors that interact with host epithelial surfaces, degrade the mucus, and promote the acquisition of essential nutrients such as carbon source [17]. Sugars are not found in a free form in the upper respiratory tract [18, 19]; instead, they are linked to the proteins (and lipids) of the epithelial cell lining and mucin [20, 21]. To benefit from the host glycoconjugates, Spn employs several glycosidases, such as Neuraminidase A (NanA), β-galactosidase (BgaA), and β-N-acetylglucosaminidase (StrH), which sequentially cleave the sugars from host glycans [21-23]. Besides supplying Spn with carbon sources, mucus degradation allows the bacteria to obstruct the mucociliary clearance. The pneumococcal autolysin LytA, promotes the release of the pore-forming pneumolysin into the extracellular environment. Ply, in turn, undermine the epithelial barriers and weaken ciliary beating.

Several adhesins facilitate pneumococcal adherence to host surfaces. Spn attachment and invasion proteins include the pneumococcal surface protein A (PspA), the fibronectin-binding proteins, PavA and PavB, and pneumococcal histidine triad protein (Pht) [15, 17]. The choline-binding proteins (CBPs) in Spn play an essential role in attachment and immune evasion. These surface proteins can bind to phosphorylcholine residues on the pneumococcal cell wall and aid in

host cell adherence [24]. CBPs can also obstruct the activation of the host complement system [15, 25]. Examples of CBPs essential for virulence include the pneumococcal surface protein A (PspA), pneumococcal surface protein C (PspC), and LytA [15, 17].

Spn establishment of infection relies on the pathogen's ability to obtain essential nutrients while in the host environment. Accordingly, many ABC importers are necessary for full virulence [26-31]. These include transporters for peptides (e.g., Ami/Ali), sugars (e.g., MalX), and cations such as zinc, manganese, and iron (e.g., Psa and Adc). Because of its role in this research project, iron hemostasis in Spn is described in more detail in a separate section below. Interestingly, the ligand-binding components of some transporters appear to have a dual role in infection; beside nutrient acquisitions, these proteins contribute to processes such as signaling, resistance to oxidative stress and adherence [15, 17, 28, 29].

1.3 Spn and iron

Iron is one of the most copious transition metals on earth and essential micronutrients for nearly all forms of life. The metal is a co-factor for many enzymes involved in critical cellular processes such as electron transport, photosynthesis, DNA synthesis, and translation. Under normal physiological conditions, the iron in the mammalian body remains in the oxidized ferric (Fe^{3+}) form, which is highly insoluble, thus needs to be bound to carrier proteins [32]. To maintain solubility, prevent toxicity, and restrict pathogen access, the mammalian host creates an iron-limited environment. Host proteins that have a high affinity for iron (for example, transferrin, lactoferrin, and ferritin) sequester all of the metal in the body. Thus, iron bioavailability is extremely low [10^{-18} M] in the host environment [33], while the growth of most bacteria demands about 10^{-6} to 10^{-7} M of iron [34, 35].

Most of the host-iron (67%) is found as heme, a heterocyclic ring that coordinates the metal iron (Fe^{2+}). Because of its lipophilic and pro-oxidant nature, heme can cause damage to cellular components such as DNA, protein, and membrane [36-38]. Therefore, mammals limit free heme in both circulation and the cellular compartment. Heme bound to hemoproteins is the primary iron pool in the body [39, 40]. The erythrocytes hemoglobin is the most abundant hemoprotein [41], and in healthy adults, its total blood concentration is approximately 1.9 to 2.3 mM [42].

Spn requires iron for growth, and like most pathogens evolved to scavenge the heme from host hemoproteins [43]. At least three ABC transporters that facilitate iron uptake (i.e., Pia, Piu, and Pit) were described in Spn [44-46]. Mutants in each system exhibit increased resistance to streptonigrin, which indicates a reduction in the cellular iron levels [44, 45, 47], and the contribution of these transporters to virulence was demonstrated in murine models [44]. The Pia transporter is carried by a pathogenicity island [44]. PiaA, the ligand-binding-protein, binds ferrichrome *in vitro*, and the structure of a PiaA-ferrichrome complex was resolved. [48]. Pneumococci, however, do not code for siderophore biosynthetic and secretion machinery [43, 49]. It is possible that Pia may function in the import of siderophores produced by the members of the nasopharyngeal microflora. PiuA, the solute-binding protein of the Piu transporter, binds heme and hemoglobin *in vitro*. A *piu* knockout mutant does not exhibit a defect in the use of hemoglobin as an iron source. Still, a *piu*/*pia* double mutant is attenuated for growth on hemoglobin iron [47]. These findings imply that both systems contribute to heme uptake. Recently, another putative lipoprotein SPD_1609 was implicated in iron-binding function like PitA [50, 51]. A knockout *spd_1609* mutant reduced adherence and invasion to host epithelial cells and decreased virulence in a mouse bacteremia model [51]. Spbhp-37, is a ligand-binding protein that binds both heme and hemoglobin with high affinity [52]. Spbhp-37 antiserum inhibits pneumococcal growth in the

presence of hemoglobin as the sole source of iron. The cytoplasmic protein Spbhp-22 was demonstrated to bind heme *in vitro*, and a mutant lacking this protein suffered from a reduced level of iron. Nevertheless, the mechanism by which Spbhp-22 mediates iron uptake remains unclear [53].

1.4 Biofilms in Spn disease

Upon colonization of the nasopharyngeal mucosa, pneumococcus forms organized multicellular communities known as biofilms. Dense aggregates of bacteria produce the biofilm matrix, which consists of proteins, DNA, and extracellular polysaccharides and facilitates adherence to biotic and abiotic surfaces [54]. Both carriage and invasive pneumococci isolates produce biofilm, and pneumococcal biofilms have been detected *in vivo*. For example, biofilms were found the biopsy specimen of adenoid cells collected from children with chronic otitis media [55], during chronic rhinosinusitis [56], and in cardiac microlesions [57]. The biofilm lifestyle helps pneumococcus escape the host immune responses [54, 58], and provides opportunities to naturally competent Spn to participate in unidirectional transformation and horizontal gene transfer conferring antibiotic resistance and the rise in new capsular variants [59]. Interestingly, Studies in Influenza A virus models suggest that altered nutrient availability in tissue prime pneumococci in biofilms to shift into the invasive planktonic state [60].

Multiple pneumococcal products are known to involve biofilms formation *in vivo*. Sialic acid was shown to act as a biofilm signal during colonization [61]. Accordingly, the pneumococcal NanA, which cleaves the terminal sialic acid from host glycoproteins in the nasopharynx, was found to play a vital role in nasopharyngeal biofilm formation [62]. An *in vivo* study in murine

infection models demonstrated that the pneumococcal serine-rich protein, PsrP, is critical for Spn persistence in the lower respiratory tract [63]. This protein facilitates intraspecies interactions that foster biofilm formation in the nasopharynx and the lungs [64].

2 CHAPTER 1: HEMOGLOBIN INDUCES GROWTH AND TRANSCRIPTOME SHIFT IN *STREPTOCOCCUS PNEUMONIAE*: A NEW PARADIGM IN PNEUMOCOCCAL HOST PATHOGEN INTERACTIONS

Streptococcus pneumoniae (Spn) must acquire iron from the host to establish infection. We examined the impact of hemoglobin, the largest iron reservoir in the body, on pneumococcal physiology. Supplementation with hemoglobin allowed Spn to resume growth in an iron-deplete medium. Pneumococcal growth with hemoglobin was unusually robust, exhibiting an extended logarithmic growth, higher biomass, and extended viability in both iron-deplete and standard medium. We observed the hemoglobin-dependent response in multiple serotypes, but not with other host proteins, free iron, or heme. Remarkably, hemoglobin induced a sizable transcriptome remodeling, effecting virulence and metabolism in particular genes that facilitate host glycoconjugates use. Accordingly, Spn was more adapted to grow on the human glycoprotein α-1 acid as a sugar source with hemoglobin. A mutant in the hemoglobin/heme-binding protein Spbhp-37 was impaired for growth on heme and hemoglobin iron and exhibited reduced growth in THYB supplemented with hemoglobin. In summary, the data show that hemoglobin is highly beneficial for Spn cultivation *in vitro* and suggest that hemoglobin might drive the pathogen adaptation *in vivo*. The hemoglobin receptor, Spbhp-37, plays a role in mediating the positive influence of hemoglobin. These novel findings provide intriguing insights into pneumococcal interactions with its obligate human host.

2.1 Introduction

Streptococcus pneumoniae (Spn) is a significant human pathogen that causes illnesses ranging in severity from common otitis media infections to invasive diseases such as pneumonia, bacteremia, and meningitis. Pneumococcal pneumonia is also a significant risk factor for the

development of cardiac diseases and heart failure [9, 10]. Altogether, the toll of Spn on human health is substantial, and the pathogen is responsible for ~15 million infections each year and about half a million deaths in children worldwide [7, 8]. Pneumococci commonly colonize the human nasopharynx and can persist asymptomatically for years in healthy individuals [1]. From the nasopharynx, Spn can be transmitted among hosts [17] and spread to other organs. Young children (<5 years of age), the elderly, and immunocompromised persons are the most susceptible individuals to pneumococcal infections [5, 6, 11]. While colonization of the upper respiratory tract is a pre-requisite for pneumococcal pathogenesis and infectivity, the factors that govern the establishment of Spn in the human host and the pathogen's transition into a virulent state, are not fully appreciated.

Spn is a dangerous pathogen that thrives in its obligate human host. *In vitro,* however, this fastidious bacterium exhibits relatively weak growth. Several studies were undertaken to optimize streptococcal cultivation in a complex (e.g., Todd-Hewitt broth containing Yeast extract (THYB) and tryptic soy broth) or defined media [65-67]. Pre-cultivation (i.e., inoculating with cells collected from a logarithmic-phase culture), medium replenishment, and growth in bioreactors with controlled growth parameters (such as pH and oxygen levels) were found to improve pneumococcal growth, although often in a strain-dependent manner [65]. Inoculating THYB with cells grown overnight in either broth or solid medium typically results in a long lag period that is followed by a relatively short exponential growth. The culture enters the stationary phase with low optical density ($O.D._{600}$ of 0.3 to 0.5, see references [45, 68] for examples). In addition to the limited biomass, Spn cultures remain viable for a much shorter time when compared to other bacteria. An autolysis mechanism that is activated upon entry into the stationary phase or in

response to inhibition of the cell-wall synthesis is often responsible for the decreased viability observed during *in vitro* cultivation. A threshold concentration of the extracellular amidase, LytA, determines the onset of autolysis. During infection, however, the cell-wall degrading LytA is needed for fratricidal lysis and virulence [69, 70]. The pneumococcal pyruvate oxidase, SpxB, and its metabolic by-product H_2O_2 also contribute to pneumococcal killing during the stationary phase of growth [71].

Within the human body, high-affinity proteins sequester iron and reduce the metal bioavailability for invading microbes in a process called nutritional immunity. During colonization and the courses of infections, pneumococci must gain access and retrieve the iron it needs for growth from host proteins that carry heme or metal iron [72-74]. Most of the metal in the human body is in heme within the erythrocyte hemoglobin (67% of the total body iron). Myoglobin and cytochrome represent most of the remaining heme pool (3.5 and 3 %). Iron is also highly sequestered in the extracellular compartment. The serum proteins hemopexin and transferrin respectively remove the small amounts of free heme and iron in the serum. The host lactoferrin sequesters ferric ions from secretions and near the infection site. Spn readily grows on heme or hemoglobin iron [43] but is unable to obtain the metal from transferrin and lactoferrin [43]. The pneumococcal mechanisms that facilitate the capture and uptake of heme are only partially understood [75, 76]. The ABC transporter PiuBCDA (also known as Pit1BCDA) is the only recognized heme importer in Spn. PiuA, the ligand-binding component, binds heme and hemoglobin *in vitro,* and inactivation of the *piuBCDA* genes partially impairs Spn growth on heme iron. [47]. Spbhp-37, is the second substrate-binding protein in Spn that interacts with hemoglobin and heme [52]. Spbhp-37 antiserum inhibits pneumococcal growth on hemoglobin iron. However,

a mutant in *spbhp-37* was not described, and it's not known which transporter works with this substrate-binding protein for heme import. A recent report implicated an additional Spn protein, Spbhp-22, in iron uptake. *In vitro* assays showed that Spbhp-22 binds heme, but the mechanism by which this cytoplasmic protein promotes iron or heme intake remains unclear [53]. Since hemoglobin is the primary source of an essential nutrient during infection, we hypothesized that hemoglobin is vital for pneumococcal pathophysiology.

2.2 Materials and Methods

2.2.1 Bacterial strains and growth media

The Spn strains used in this study are listed in Table 2.1. Frozen Spn stocks were prepared in the medium Skim milk-Tryptone-Glucose-Glycerin (STGG) as described [77] and kept at -80 °C. Spn STGG stocks were plated on Tryptic Soy blood agar plates (BAPs) and incubated overnight at 37°C under microaerophilic conditions. Spn was also grown in Todd-Hewitt broth containing 0.5% (w/vol) Yeast extract (THYB) or in Casein-Tryptone (CAT) medium [78] containing Bacto Casitone 10 g/l, Bacto Tryptone 10 g/l, Yeast extract 1 g/l, NaCl 5 g/l, 0.5M K_2HPO_4 (30 ml/l) and 200 U/µl of catalase. One or more of the following supplements were added to the growth medium as indicated: The iron chelator 2, 2'-Di-pyridyl (Acros organics), bovine hemin (Sigma Aldrich), human hemoglobin (Sigma Aldrich), Ferric nitrate nonahydrate ($FeNO_3$, Fisher Scientific), bovine serum albumin (BSA, Sigma Aldrich), 200 U/µl of catalase (Sigma Aldrich), glucose (Sigma Aldrich), human α-1 acid glycoprotein (AGP, Sigma Aldrich), or fatty-acid free human serum albumin (Sigma Aldrich). Some experiments used frozen logarithmic Spn stocks as the starting inoculum. To prepare such stocks, Spn cells growing in THYB were collected

at the early logarithmic phase of growth ($O.D._{600}$ = 0.2-0.3), and glycerol was added to the culture to a final 10% (vol/vol) and stored at -80 °C.

2.2.2 The growth assays

Fresh medium (with or without supplements) was inoculated with Spn cells collected from BAPs following overnight incubation (starting $O.D._{600}$ = 0.05) or from frozen logarithmic culture (starting culture $O.D._{600}$ = 0.02) as indicated. Cell cultures (200 µl per well) were allowed to grow in 96-well microtiter plates (Corning) incubated at 37 ˚C. The culture $O.D._{600}$ was recorded at 1hour intervals for 18 hours using a SpectraMax M2 spectrophotometer (Molecular Device). For each growth condition, we used wells containing only the medium (and supplements when appropriate) as the blank. Bacterial growth was tested in triplicates. To determine cell viability, culture samples were collected at designated time points, serially diluted in 0.9% saline, and plated in triplicates into BAP.

2.2.3 Total iron determination by ICP-MS

Fresh THYB medium containing 80 µM $FeNO_3$ or 20 µM hemoglobin was inoculated with Spn grown on BAPs (starting $O.D._{600}$ = 0.05) and incubated at 37 °C for 6 h in 12 well microtiter plates. Culture samples (6 ml, $O.D._{600}$ = 1) were washed three times with phosphate-buffered saline (PBS) prior to collection. The cell pellet was digested and analyzed (Center for Applied Isotope Studies, University of Georgia, Athens, GA) as described [79, 80].

2.2.4 Construction of Δspbhp-37 mutant

The plasmids used in this study are listed in Table 2.1 and the primers in Table 2.2. We cloned a Δ*spbhp-37* mutant in Spn strain D39 by replacing the *spbhp-37* coding sequence with that of *ermB* (erythromycin resistance [81]), such that the *ermB* ORF is under the transcriptional control of *spbhp-37* promoter and terminator. The mutant allele containing *ermB* ORF flanked by the 5' and 3' genomic regions of the *spbhp-37* gene was prepared using the Gene art seamless cloning kit (Thermo fisher scientific). Briefly, the appropriate genomic segments were amplified from D39 chromosome using the primer sets ZE 740-L/ZE 741-R and ZE 744-L/ZE 745-R. The *ermB* gene and the pUC19 vector were amplified from pCR2.1 topo and pUC19-L plasmids using the primer sets ZE 742-L/ZE 743-R and ZE 738-L/ZE 739-R, respectively. All PCR fragments were purified (using the Minelute PCR purification kit, Qiagen) and cloned into One-shot topo *E. coli* strain, generating plasmid pAF104. The resulting allele was then amplified (from pAF104) and transformed into competent D39 cells using standard protocols [82]. The mutants were selected on BAPs containing erythromycin (0.5 µg/ml). The mutation was confirmed by PCR in the resulting erythromycin-resistant clones using the primer set ZE 740-L/ZE 745-R.

2.2.5 Spn growth with human α-1 acid glycoprotein and serum albumin

To remove contaminating free sugars, human α-1 acid glycoprotein (AGP, 10 mg/ml) was dialyzed in water using Slide-A-Lyzer dialysis cassette G2 (10,000 molecular weight cutoff, Thermo scientific) as described [22]. The samples were then concentrated with Amicon Ultra centrifugal filters (MWCO 10,000), reconstituted in CAT medium (5 mg/ml) and filter sterilized. Spn D39 grown overnight on BAP were collected, washed and suspended in CAT. These cell suspensions were used to inoculate fresh CAT medium with or without glucose (0.5% (w/v), AGP

(5 mg/ml) or HSA (20 μM). Bacterial growth in the presence or absence of 20 μM hemoglobin in 96-well microtiter plates was monitored as described above.

2.2.6 RNA-Seq analysis

Fresh THYB was inoculated with Spn cells from frozen logarithmic stocks (starting culture $O.D._{600}$ = 0.02) and the cultures were allowed to grow in 12 well microtiter plates (2 ml per well) at 37 °C. 20 μM Hb (in 0.9% saline) or 0.9% saline (negative control) was added to the growing cells at the early logarithmic phase ($O.D._{600}$ = 0.2-0.3). Cultures samples (four biological replicates for each condition) were collected and mixed with RNA protect reagent (Qiagen) following manufacturer's recommendations. Cells were then collected by centrifugation and stored at -80 °C. For RNA preparation, cell samples were suspended in 700 μl of Trizol with 300 mg of acid-washed glass beads (Sigma Life Science) and disrupted by vortexing. Total RNA was isolated using the Direct-zol RNA MiniPrep kit (Zymo Research). DNA was removed using the Turbo DNase-free kit (Life Technologies). rRNA was eliminated with the Ribo-Zero Magnetic kit for Gram-positive bacteria (Epicenter). RNA Quality and quantity were assessed using a 2100 Bioanalyzer (Agilent) and NanoDrop 8000 spectrophotometer (Thermo Scientific), respectively. Directional RNA-Seq libraries were created using the ScriptSeq v2 RNA-Seq Library Preparation kit (Illumina) according to the manufacturer's instructions. A rapid-run 100 bp single-read DNA sequencing was performed at the Institute for Bioscience and Biotechnology Research (IBBR) Sequencing Facility at the University of Maryland, College Park, using the Illumina HiSeq 1500 platform. Data were generated in the standard Sanger FastQ format and raw reads were deposited with the Sequence Read Archive (SRA) at the National Center for Biotechnology Institute (accession PRJNA626052). Read quality was evaluated using FastQC software (Babraham

Bioinformatics), and mapping against the Spn D39 genome using Bowtie package alignment software [83]. The read count or raw count data for all genes were acquired using Feature count package [84]. These raw count data files were then used in DESeq2 package [85] to calculate differential expression analysis of all samples for pairwise comparison. Graph Pad Prism (version 8.3.1) was used to prepare dot plot representation of gene expression levels using normalized RNA-seq read counts.

2.2.7 qRT-PCR analysis

Quantitative reverse transcription PCR (qRT-PCR) analysis was carried out using the Power SYBR® Green RNA-to-Ct™ 1-Step Kit (AB) and 7500 Fast Real-Time PCR machine (AB) according to the manufacturer's specifications. A total of 25 ng RNA was used per qRT-PCR reactions and each reaction was done in duplicates. Primers used for qRT-PCR are listed in Table 2. The relative expression was normalized to the endogenous control *gyrB* gene and fold changes were calculated using the comparative $2^{-\Delta\Delta CT}$ method.

2.3 Results

2.3.1 Hemoglobin stimulates unusually robust growth of Spn in batch cultures

To test the use of hemoglobin iron by Spn, we adopted the growth assay from our studies with the related Group A Streptococcus [86]. We cultivated Spn in fresh THYB, with or without the iron chelator 2, 2'-Di-pyridyl (DP) and different iron supplements (Fig. 2.1). Spn did not grow in THYB-DP, but growth was restored when we complemented the medium with ferric iron (≥ 0.5 mM, Fig. 2.1A), demonstrating that DP prevents pneumococcal cultivation by limiting iron bioavailability. Supplementation with hemoglobin (Fig. 2.1B) or heme (Fig. 2.1C) also supported

Spn growth in THYB-DP in a dose-dependent manner. Higher amounts of $FeNO_3$ compared to a heme source (mM vs. μM, respectively) were needed to support growth, because DP chelates metal iron but not heme [86, 87]. Surprisingly, hemoglobin facilitated a much better growth THYB-DP compared with free iron (Fig. 2.1B). In the presence of hemoglobin, the culture displayed only a brief lag phase, which was followed by a prolonged (and somewhat bi-phasic) exponential period, reaching a higher maximal optical density. Free heme also supports Spn growth in THYB-DP, but growth was not as robust as with hemoglobin, and heme became a growth-inhibitory above ten μM (Fig. 2.1C).

Spn growth in THYB-DP with hemoglobin (≥ 5 μM) exceeded the one observed in standard medium (THYB, Fig. 2.1A & B). We tested the impact of adding 0.5 - 20 μM hemoglobin to iron complete THYB. Remarkably, hemoglobin stirred vigorous growth in a dose-dependent manner (Fig. 2.2A). Incubation with 20 μM serum albumin, which has a similar molecular weight (~60 kDa), resulted only in a minimal growth improvement (Fig. 2.2B). Supplementation with hemoglobin that was heat-inactivated did not promote growth. To rule out the possibility that a contaminant in our hemoglobin preparation was responsible for the observed enhanced growth, we filtered the hemoglobin solution using 10,000 MW cutoff and tested both fractions for growth impact. The filtered hemoglobin retained activity while the flow-through was somewhat growth-inhibitory (Fig. 2.2B). It seemed possible that the positive growth induced by hemoglobin results from the intrinsic peroxidase activity of hemoglobin [88], leading to protection from hydrogen peroxide [89]. To test this hypothesis, we grew Spn in THYB and added catalase to scavenge hydrogen peroxide. Results in Fig. 2.2C demonstrate that supplementation with catalase had a minimal impact on Spn cultivation.

Supplementation with an equimolar amount of iron (10-80 μM $FeNO_3$, each hemoglobin molecule has four heme groups) did not have a significant effect (Fig. 2.2D). The addition of free heme to THYB did not improve growth at the low μM range and was inhibitory above ten μM (Fig. 2.2E). To evaluate whether the enhanced growth was due to an improved uptake of iron when pneumococci are incubated with hemoglobin, we measured intracellular iron levels by ICP-MS (Fig. 2.2F). Equal amounts of iron were found in cells grown in THYB or THYB with 20 μM hemoglobin. Surprisingly, supplementation with 80 μM $FeNO_3$ resulted in an actual reduction in the total iron cellular level.

We next tested the viability of cells at different time points during growth in THYB with and without 20 μM hemoglobin. Consistent with the higher optical density, in the presence of hemoglobin, viable count at 8-hour post-inoculation was about twice as that determined for cultures grown without hemoglobin (Table 2.3). Cells exhibited a sharp decline in viability after overnight incubation (18 hours) in both THYB and THYB with hemoglobin. However, 18-fold more viable cells were obtained in cultures grown with hemoglobin compared to cultures cultivated in THYB alone (Table 2.3, 18 h). In summary, hemoglobin-induced growth and viability are a hemoglobin-dependent phenomenon observed in both iron-deplete and iron-complete medium.

2.3.2 Hemoglobin modulates Spn growth independently of the strain and the growth assay

Next, we asked if the response to hemoglobin is widespread among pneumococcal strains, and thereby tested the impact of hemoglobin on TIGR4 and two clinical isolates. These

experiments revealed that hemoglobin stimulated growth in all three strains (Fig. 2.3A). The positive impact of hemoglobin might only be seen in our experimental system whereby Spn are grown on blood agar plates prior to inoculating THYB. To examine if this is the case, we inoculated fresh THYB with an overnight culture grown in THYB (Fig. 2.3B). Compared to cells collected from BAPs, bacteria that came from liquid culture (in THYB) exhibited a more prolonged lag phase and yielded lower final biomass. Nonetheless, the addition of hemoglobin still significantly improved the second round of growth in THYB in these cells. We next used frozen logarithmic cells grown in THYB to start new THYB cultures with and without hemoglobin (Fig. 2.3B). Inoculating the medium with logarithmic cells abolished the lag phase and improved overall growth. Still, supplementation with hemoglobin enhanced growth even further compared to THYB alone. We also tested the effect of hemoglobin on pneumococcal growth in casein tryptone (CAT) medium. When we inoculated CAT medium with Spn cells collected from BAPs, the bacterial growth was comparable to the one seen in THYB inoculated with cells from BAPs. The addition of hemoglobin to CAT, however, altered the bacterial growth pattern and yield. In the presence of hemoglobin, the pneumococci exhibited only limited growth for the first six hours in CAT. This initial phase was followed by extended exponential growth that resulted in higher biomass compared to pneumococci growing in CAT only (Fig. 2.3C). In summary, hemoglobin dramatically impacts growth in batch cultures of multiple pneumococcal strains regardless of the assay, or media used.

2.3.3 Hemoglobin induced a sizable transcriptome remodeling

Since hemoglobin has a considerable influence on growth, we asked how it may affect pneumococcal gene expression. Hemoglobin or saline (as a control) was added to Spn cultures

grown in THYB at the early log phase and culture samples were collected one- and two-hours post-treatment. RNA was isolated from four biological replicates for each growth condition and analyzed by RNA-Seq. This global transcriptome study revealed that the addition of hemoglobin to the growth medium resulted in a significant shift in gene expression. 59 Spn genes were upregulated and 18 genes were down-regulated (at least two folds) in response to hemoglobin within one hour (Fig. 2.4A & B), and a total of 100 and 45 genes were induced or repressed respectively two hours post-treatment. qRT-PCR on a subset of regulated genes validated the RNA seq findings (Appendix A).

Many of the genes that were differentially expressed in response to hemoglobin are related to the import and biosynthesis of nucleotides, amino acids, fatty acids, and lipids (Fig. 2.5). Notably, hemoglobin activated the transcription of several metabolic genes and genes encoding virulence factors needed for Spn nasopharyngeal colonization and infections. These include the genes of the oligopeptide-binding proteins, *aliA* and *aliB* [28], the PGN hydrolase, *lytB* [90], the gene encoding the pneumococcal histidine triad protein D, *phtD* [91] and the surface adhesin, *pavB* (Fig. 2.5A) [92]. Hemoglobin also repressed many metabolic genes of which, it is noteworthy that the whole operon coding for proteins of a heme importer, *piuBCDA*, was downregulated by incubation with hemoglobin (SPD_1649-52, Fig. 2.5B) [44]. The expression of the heme/hemoglobin binding protein, *spbhp-37*, which also promotes Spn use of hemoglobin iron [52, 93], was high but not differentially expressed (Fig. 2.5C).

Many of the hemoglobin-responding genes are related to carbohydrate intake and conversion (Fig. 2.6). The *bgu* operon [94] encoding a lactose type phosphotransferase system (PTS) (SPD_1830-33) exhibited the most robust induction post hemoglobin addition (6-fold and

16-25-fold in the first and second hours respectively, Fig. 2.6A). *In vitro*, this PTS system mediates the use of beta-glucosides such as amygdalin or cellobiose [95]. During infection, however, β-linked disaccharides found in glycosaminoglycans of the host extracellular matrix are the proposed substrates of the *bgu* PTS. Other hemoglobin responding loci involved in carbohydrate metabolism include the *lacABCD* genes (SPD_1050-54, the tagatose pathway enzymes), *bgaA* and *bgaC* enzymes, and the associated galactose and mannose type PTS systems (SPD_0559-62 and 0067-71 respectively). A mannose-type PTS system (SPD_0293-5) that is involved in the use of sulfated-glycosaminoglycan (e.g., hyaluronic acid) [95] was upregulated in second hour of hemoglobin treatment (Fig. 2.6A). In contrast, hemoglobin downregulated the expression of the ABC transporter (*rafGFE*) that imports the trisaccharide raffinose and of a glycerol facilitator (Fig. 2.6B).

2.3.4 Hemoglobin promotes pneumococcal growth on host glycoconjugates in vitro

Since hemoglobin induced the expression of PTSs and enzymes that are known or predicted to be involved in the use of host glycans, we hypothesized that hemoglobin enhances the ability of Spn to use these host molecules as nutrients. To test this hypothesis, we examined the impact of hemoglobin on Spn growth on the human α-1-acid glycoprotein, AGP (N-linked glycan, Fig. 2.7A). Spn growth in CAT medium (which contains glucose) was similar to that seen in THYB (Fig. 2.3C). The removal of the glucose from the CAT broth, however, impeded growth (Fig. 2.7B). Spn grew rapidly when the sugar-free CAT was supplemented with both AGP and hemoglobin, but not in sugar-free CAT medium supplemented with either AGP or hemoglobin individually (Fig. 2.7B). The addition of human serum albumin as a control did not promote growth in sugar-free CAT with or without AGP (Fig. 2.7C). These data indicate that hemoglobin

promotes pneumococcal use of AGP *in vitro* and suggests it may enhance the use of host glycoproteins as a carbohydrate source *in vivo*.

2.3.5 A spbhp-37 deletion mutant exhibits a lessened growth response to hemoglobin

Although hemoglobin stimulates Spn growth in both iron-complete and iron-deplete THYB, it still seemed possible that the positive influence of hemoglobin is related to its ability to donate heme. THYB supplementation with hemoglobin repressed transcription of the heme importer genes *piuBCDA*, allowing for only very low expression (Fig 2.5C). The expression of *spbhp-37*, the second heme/hemoglobin receptor with a role in heme uptake, however, was high (with and without hemoglobin Fig. 2.5C). *In silico* analysis predicted that Spbhp-37 is expressed as a monocistronic mRNA [96]. To see if Spbhp-37 plays a role in the response, we generated a deletion mutant (replacing *spbhp-37* ORF with that of *ermB)* and tested its impact on hemoglobin growth induction (Fig. 2.8). The Δ*spbhp-37* mutant was not able to grow in THYB-DP supplemented with free heme and exhibited growth attenuation when grown in THYB-DP supplemented with hemoglobin (Fig. 2.8A). The mutant also had a growth phenotype in THYB alone. Although Δ*spbhp-37* growth was improved in the presence of hemoglobin, it was still reduced compared with the wild type strain (Fig. 2.8B). ICP-MS analysis demonstrated a significant reduction in total iron levels in the Δ*spbhp-37* compare with the parental strain in cells grown in THYB with 20 μM hemoglobin (Fig. 2.8C). These observations confirm a role for Spbhp-37 in iron uptake and imply that this hemoglobin/heme-binding protein plays some role in the Spn growth response to hemoglobin.

2.4 Discussion

In this study, we demonstrated that hemoglobin, a host hemoprotein, has a substantial impact on Spn physiology and planktonic growth. The data reveal that the presence of hemoglobin greatly benefits pneumococcal growth and viability in complex laboratory media, redirecting the pneumococcal transcriptome and metabolic capacity. This appears to enhance the ability of Spn to use host glycoproteins as a source of carbohydrates, providing a potential fitness advantage during colonization and infection. The data also suggest that the heme uptake protein, Spbhp-37, plays a role in the positive influence of hemoglobin on Spn physiology. Below we discuss how these intriguing findings advance our current understanding of Spn interactions with its obligate human host.

Hemoglobin facilitates vigorous growth in iron-depleted medium. The reinstatement of Spn growth in the iron-depleted medium, THYB-DP, by hemoglobin or heme (Fig. 2.1B & C) shows that Spn can metabolize heme iron, as it was previously reported [43, 44, 52]. Hemoglobin iron, however, appears particularly beneficial, triggering strong Spn growth surpassing that seen with free iron or heme alone (Fig. 2.1). This is the first report to describe the unusually robust growth of Spn upon hemoglobin supplementation in an otherwise iron-deplete medium. Why had other investigators not seen this exquisite hemoglobin-specific enhanced growth? Technical differences, such as the use of the chelating resin, Chelex-100, might have masked the positive impact of hemoglobin in prior investigations [43, 44, 52]. Chelex-100 has broad specificity, and treatment with this resin might have limited the availability of additional cations that are needed for full Spn growth. Furthermore, the long pre-cultivation in iron-deprived medium prior to the

addition of hemoglobin used in some studies [52], might also have limited maximal growth with hemoglobin.

THYB-DP supplemented with heme above 5-10 μM (equivalent to 20-40 μM hemoglobin) was growth inhibitory. In excess, heme is harmful to many bacteria, including the related *Streptococcus pyogenes*, due to its lipophilic and oxidative nature, which damages the bacterial membranes, proteins, and nucleic acids [97, 98]. The negative impact that is inherent to the presence of free heme in the medium may prevent the benefit of heme that is provided by hemoglobin. Hemoglobin likely delivers the heme directly to surface receptors and membrane transporters for import [47, 93, 99]. Compared to free heme, heme that is delivered from one protein to another likely has fewer opportunities to damage the cell envelope.

Spn growth stimulation is hemoglobin-dependent and utilizes a unique mechanism. Supplementing THYB with hemoglobin enhances pneumococcal growth, shortening the lag period, and increasing maximal biomass and viability (Fig. 2.2A & B and Table 2.3). Other host proteins, inactivated hemoglobin, or the flow-through collected after hemoglobin filtration, did not have this effect. Hence, it is hemoglobin in its native form, rather than a nonspecific increase in peptides and amino acids availability, or the presence of low molecular weight contaminants, that is advantageous for Spn growth. Spn is often grown with a source of catalase (e.g., blood) to neutralize a large amount of hydrogen peroxide this bacterium can produce. If inhibition of H_2O_2 by hemoglobin allowed enhanced growth, then the addition of catalase to THYB would have improved growth, but this did not occur (Fig. 2.2C), suggesting that hemoglobin does not extend growth by scavenging the H_2O_2 from the medium.

Supplementation with ferric iron did not enhance Spn growth in THYB, suggesting that the iron levels in this medium are not growth-limiting for Spn (Fig. 2.2D). Moreover, the cellular levels of iron in cells grown in THYB with hemoglobin are similar to those found in cells grown in regular THYB (Fig. 2.2F). Therefore, hemoglobin growth benefits are not derived by facilitating an increase in the total iron level in Spn. Hemoglobin, however, might have increased the cellular heme-to-iron ratio compared with cells that grew in THYB. Hence, we speculate that hemoglobin promotes growth, at least in part, by donating heme and that heme is more growth beneficial then metal iron. The finding that Spn imports less of the metal when THYB is enriched with ferric iron (Fig. 2.2F) supports the idea that heme might be more useful for the pathogen's physiology than free iron. Other pathogenic bacteria such as *Staphylococcus aureus* and *S. pyogenes* demonstrate a preference for heme when supplied with both free iron and heme [100, 101]. Canonical heme degradation results in the production of biliverdin and its reduced product bilirubin [102], both molecules scavenge various ROS and are considered potent antioxidants [103, 104]. Perhaps, similar to the human host, heme catabolism by Spn leads to the production of protective end products and thus is valuable beyond iron release. Studies in our laboratories are underway to address this hypothesis.

The positive response to hemoglobin was rigorously assessed in the current study and found to be shared by multiple pneumococcal strains and independent of the growth assay used (Fig. 2.3). The addition of hemoglobin shortens the lag period in THYB inoculated with overnight cultures that grew either on BAPs or in THYB (Fig. 2.3B). Nevertheless, cells that were collected from BAPs exhibited improved growth. It's possible that the presence of hemoglobin is one of the growth-promoting factors in BAPs, which are commonly used for Spn cultivation. Notably, the addition of hemoglobin to THYB inoculated with logarithmic cells still enhanced growth (Fig.

2.3B). Hence, hemoglobin acts by both stimulating growth in resting cells and by extending the growth period before an exponentially growing culture enter the stationary phase. Spn growth with hemoglobin appeared biphasic in all conditions, other than in cultures inoculated with logarithmic cells. The formation of a two-step growth curve was more apparent in the experiments using Spn grown on THYB as the inoculum (Fig. 2.3B), in CAT medium (Fig. 2.3C), and with the Δ*spbhp-37* mutant (Fig. 2.8A & B). We have not explored in detail this biphasic growth pattern. Still, the absence of the first growth phase in cultures using logarithmic cultures implies that the initial hemoglobin impact on resting cells can be separated from its influence on exponentially growing cells.

It is not fully understood why Spn exhibits limited growth in batch cultures and enters early into the stationary phase. Acidification and other growth conditions were implicated as growth limiting factors. Nevertheless, at least some Spn strains (such as D39), still demonstrated limited exponential growth even under conditions where the pH and other factors such as temperature and atmosphere were controlled [65, 105]. The data here show that hemoglobin extends Spn growth in medium that was not otherwise replenished, without pH control, with or without pre-cultivation. Therefore, it's possible that hemoglobin (directly and/or via the heme it donates) redirects a regulatory mechanism(s) that otherwise leads to premature growth arrest during *in vitro* cultivation. Interestingly, hemoglobin did not influence the expression of *lytA* and *spxB,* which cause Spn death, but the expression of these two genes was high under our experimental conditions (Fig. 2.6C). It is worth noting that for our transcriptome studies hemoglobin was added at the early exponential growth, and gene expression was analyzed one and two hours after treatment; thus, we can't rule out a later change in *lytA* and *spxB* expression.

Hemoglobin has a broad impact on Spn transcriptome suggesting host adaptation. Hemoglobin triggered significant transcriptome remodeling (Fig. 2.4). Various genes with an established role in colonization were activated (Fig. 2.5A), including the *aliA/aliB* genes. The lipoproteins, AliA, and AliB, are paralogs of AmiA, the oligopeptide-binding component of the Ami system, which is used by the auxotroph Spn to import oligopeptides. [106]. Inactivation of *ami-aliA/aliB* attenuates adherence to pulmonary epithelial cells [107], and these proteins are important for the initial colonization of the nasopharynx [28]. Hemoglobin also induced the PGN hydrolase gene, *lytB,* whose activity is necessary for the adherence and invasion of human lung epithelial cells [90]. The colonizing factor PavB also positively responded to hemoglobin. PavB contributes to nasopharyngeal colonization and is highly expressed during heart infection [57, 92]. Similarly, hemoglobin induced the arginine biosynthesis genes, *argGH,* which are needed for growth in the lung, blood, and cerebrospinal fluids [108]. Hence, Spn transcriptome response to hemoglobin suggests the pathogen perceives the presence of hemoglobin as a cue for the host environment.

Hemoglobin activates pneumococcal utilization of glycoproteins found in the host mucin and the epithelial mucosa. Hemoglobin had a strong influence on the expression of many genes involved in the uptake and use of host-derived sugars found in the mucosa and extracellular matrix (Fig. 2.6). Spn can ferment about 32 different carbohydrates *in vitro* [95], and over 30% of the transporters in the Spn genome are dedicated to carbohydrate uptake [49], many of which contribute to colonization and pathogenesis. Free sugars, however, are not typically available in the upper respiratory tract [18, 19]; rather, they are linked to the glycoproteins (i.e., O- and N-linked glycan and glycosaminoglycan) found on the epithelial cell lining and in mucin [20, 21]. Sequential deglycosylation by various pneumococcal exo-glycosidases (e.g., BgaA, BgaC, NanA,

NanB and StrH) allow Spn to cleave the sugars from the host glycan for uptake ([21-23] and Fig. 2.7A). Our transcriptome analysis suggests that hemoglobin activates the expression of genes needed for the release, import, or catabolism of the host glycan derived monosaccharides, galactose and mannose, glycosaminoglycan disaccharides (e.g., hyaluronic acid), and the beta-glucosides amygdalin and cellobiose (Fig. 2.6A). Therefore, like mucin [109], hemoglobin induces the expression of Spn genes required for growth on sugars derived from the host glycans. *In vitro* growth assays confirmed that Spn could use the human α-1-acid glycoprotein AGP (N-linked glycan) as a carbohydrate source when grown in the presence of hemoglobin (Fig. 2.7B), but not in the presence of human serum albumin, HSA, as a control (Fig. 2.7C). Hemoglobin downregulated the operons encoding the glycerol MIP family transporter, *glp*, and the raffinose transporter (Fig. 2.6B). Interestingly, Spn ear isolates demonstrate a reduced capacity to use the sugar raffinose comparing with blood isolates [110].

The hemoglobin/heme receptor Spbhp-3*7* has a redundant role in mediating the hemoglobin growth benefits. PiuA and Spbhp-3*7* are the only two hemoglobin (and heme) receptors with an established role in heme uptake. Hemoglobin, however, represses expression of the *piuBCDA* transporter, while the expression of *spbhp-37* remained high whether hemoglobin was added or not (more than 30-fold above *piuA*, Fig. 2.5C). Using a *Δspbhp-37* mutant, we showed that Spbhp-37 plays an important role in the use of heme and hemoglobin iron (Fig. 2.8A). This is consistent with the observation that inhibition of Spbhp-37 by antibody interfered with Spn growth on hemoglobin iron [52]. Spn, however, was still able to utilize hemoglobin, likely due to redundancy in heme uptake systems. Notably, the *Δspbhp-37* mutant did not grow well in THYB, the addition of hemoglobin improved growth only partially, and lower iron levels were found in mutant cells grown in THYB with hemoglobin (Fig. 2.8C). Together, these observations suggest

that Spbhp-37 has a redundant role in mediating the growth benefit of hemoglobin, possibly by capturing heme from hemoglobin.

Spn is listed as a severe threat in the 2019 CDC antimicrobial-resistant (AMR) report [111]. Therefore, it is critical to gain insights into Spn pathophysiology to better design new treatment modalities. Herein, we have demonstrated that hemoglobin greatly benefits pneumococcal cultivation *in vitro*, promoting growth and viability, and causes a transcriptome shift that is likely to advance Spn preparation for colonization and infection. Hence, this study makes significant contributions to the understanding of pneumococcal growth requirements and adaptation to its obligate human host. Additional work is needed to describe the mechanism by which Spn perceives and responds to hemoglobin and the effect of hemoglobin on Spn during infection.

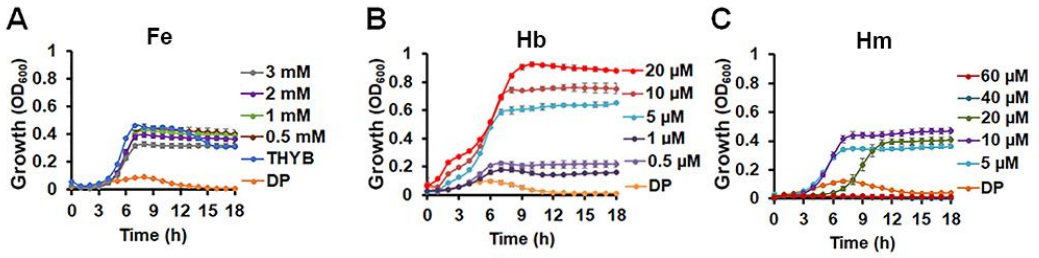

Figure 2.1: Hemoglobin-dependent growth of Spn D39 in iron-deplete medium.

THYB was inoculated with D39 cells grown on BAPs (18 h, starting $O.D._{600}$ = 0.05). Shown is growth in **(A)** THYB, THYB with 3mM di-pyridyl (DP), THYB with DP and 0.5 - 3 mM of $FeNO_3$ (Fe); **(B)** THYB with DP supplemented with 0.5 µM -20 µM hemoglobin (Hb); and

(C) THYB with DP supplemented with 5 - 60 µM heme (Hm). The data are representative of three independent experiments performed in triplicates; error bars indicate SD.

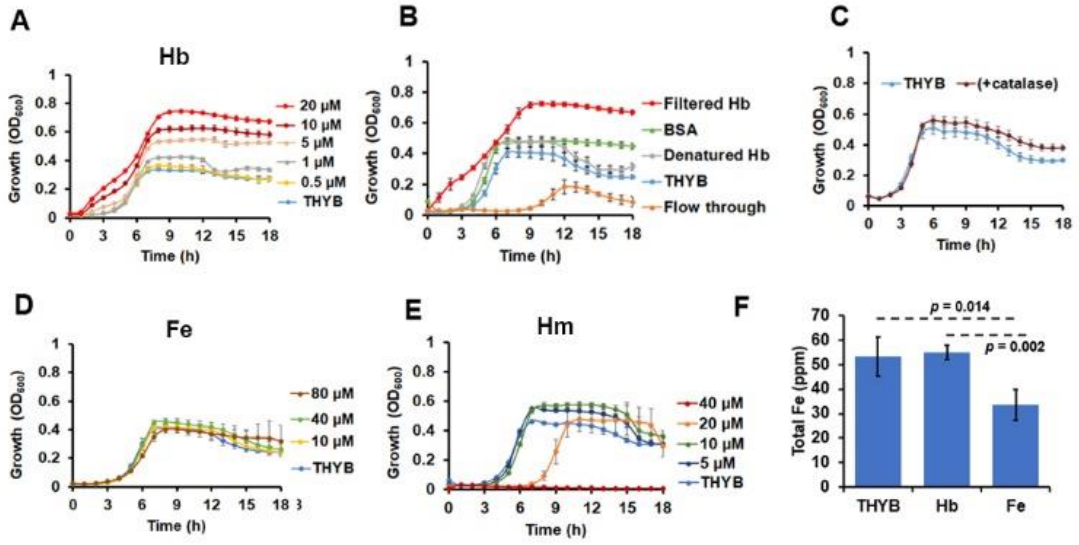

Figure 2.2: Hemoglobin stimulates a robust growth of Spn D39 in standard (iron-complete) medium.

THYB was inoculated with D39 cells grown on BAPs (18 h, starting $O.D._{600}$ = 0.05. Shown is growth in **(A)** THYB with 0 - 20 µM hemoglobin (Hb); **(B)** THYB with 20 µM BSA, denatured hemoglobin, filtered hemoglobin, or the flow-through; **(C)** THYB with or without catalase. **(D)** THYB supplemented with 0 - 80 µM $FeNO_3$ (Fe); **(E)** THYB with 0 - 40 µM heme (Hm). The data are representative of three independent experiments performed in triplicates; error bars indicate SD. **(F)** Total intracellular iron content measured by ICP-MS in culture samples (normalized to optical density) grown in THYB, THYB with 20 µM hemoglobin (Hb), or THYB

with 80 µM $FeNO_3$ (Fe). The data represents the average of three independent biological replicates; error bars indicate SD.

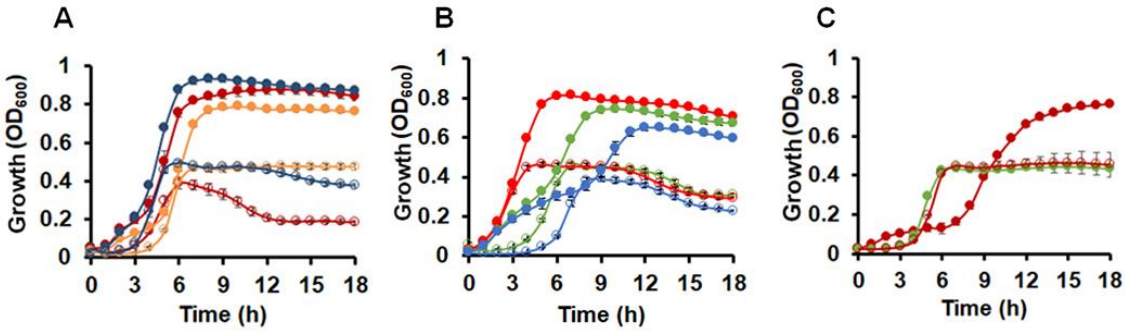

Figure 2.3: Hemoglobin stimulates Spn growth independently of the strain or the growth assay.

Shown is Spn growth in fresh THYB (empty symbols) or THYB with 20 µM hemoglobin (full symbols). The culture starting $O.D._{600}$ is indicated. (**A)** TIGR4 (red), and the clinical isolates 3875 (blue), and 8655 (yellow) grown on BAPs (18 h) was used as the inoculum ($O.D._{600}$ = 0.05). **(B)** THYB was inoculated with D39 cells from frozen logarithmic cultures ($O.D._{600}$ = 0.02, red), THYB cultures (18 h, $O.D._{600}$ = 0.05, blue), or cell from BAPs (18 h, $O.D._{600}$ = 0.05, green). **(C)** D39 growth in CAT medium (empty symbols), CAT medium with 20 µM hemoglobin (red, full symbols) or 20 µM human serum albumin (green, full symbols). The data are representative of three independent experiments performed in triplicates; error bars indicates SD.

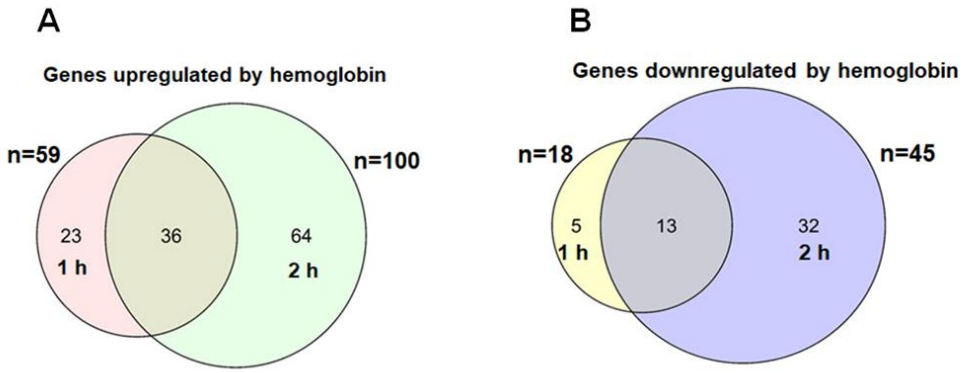

Figure 2.4: The addition of hemoglobin to the culture medium triggers a significant transcriptome remodeling in Spn.

Venn diagram (using R) of differentially expressed genes in D39 culture (fold change ≥ 2). **(A)** Genes upregulated by hemoglobin. **(B)** Genes downregulated by hemoglobin.

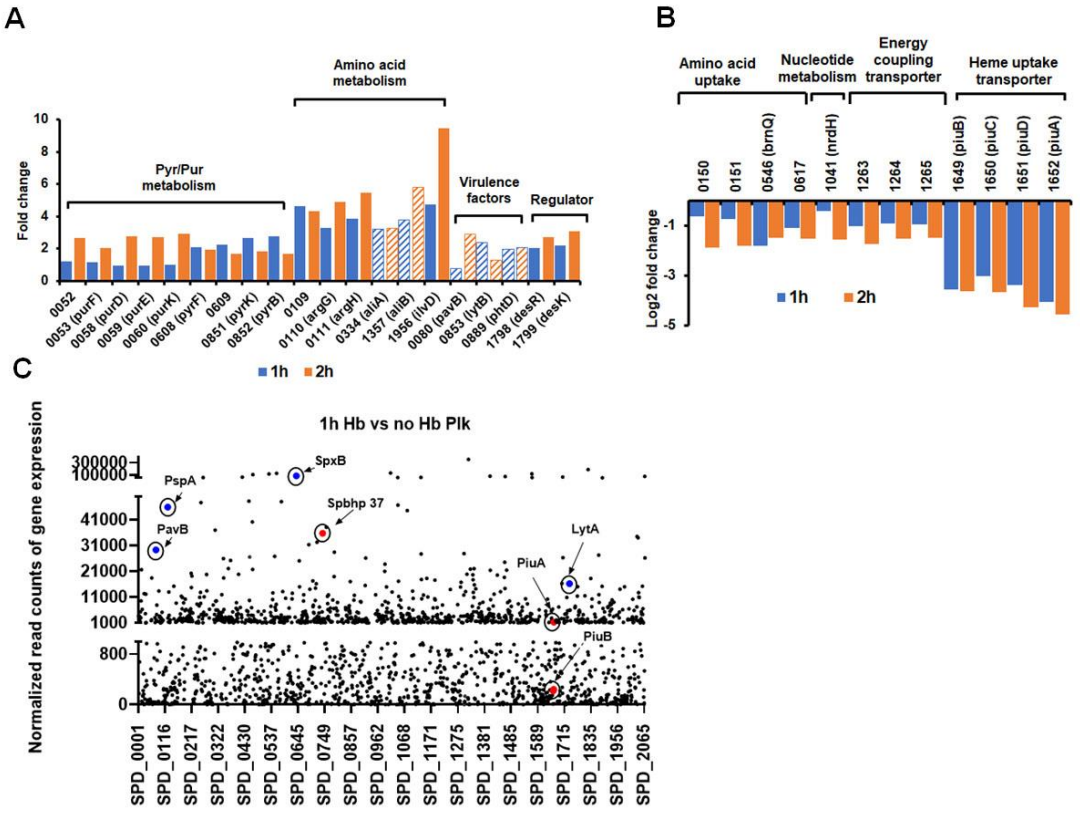

Figure 2.5: Hemoglobin activates Spn genes vital for host colonization.

The relative expression of genes involved in metabolism, nutrient uptake, virulence, or regulation, at 1 h and 2 h post hemoglobin addition (Y-axis) is plotted for D39 genes (X-axis). (**A)** Up-regulated genes. Stripes indicate involvement in nasopharyngeal colonization. **(B)** Down-regulated genes. **(C)** Dot plot representation of gene expression levels depicting normalized RNA-seq read counts (Y-axis) for cells with 1h post-treatment. Genes encoding heme/hemoglobin binding (red) or virulence factors (blue) are highlighted.

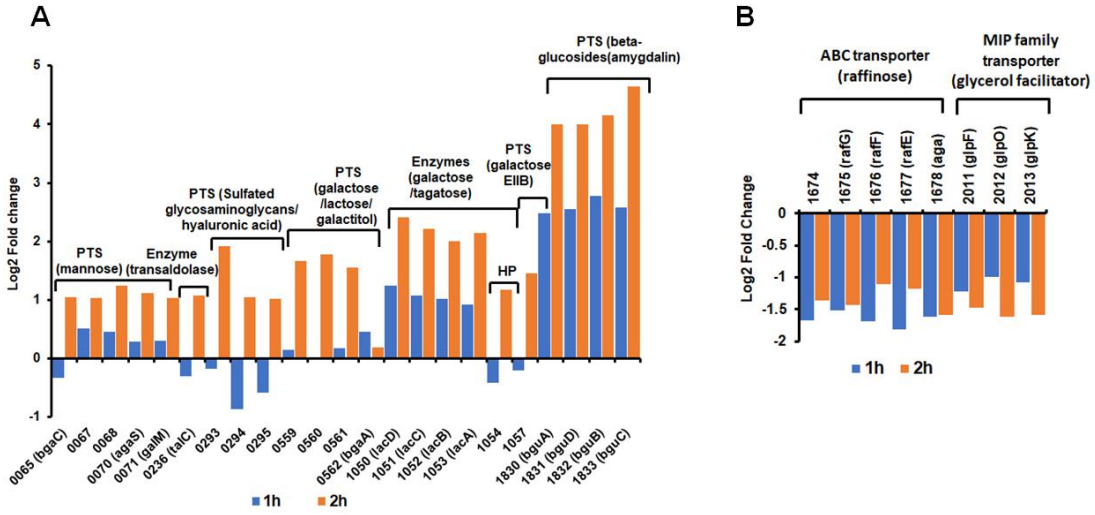

Figure 2.6: Hemoglobin up regulates Spn genes involved in host glycoconjugate use.

Log_2-fold changes in gene expression levels (Y-axis) is plotted for D39 genes (X-axis). **(A)** PTSs, enzymes and hypothetical protein (HP). **(B)** down regulated sugar transporters.

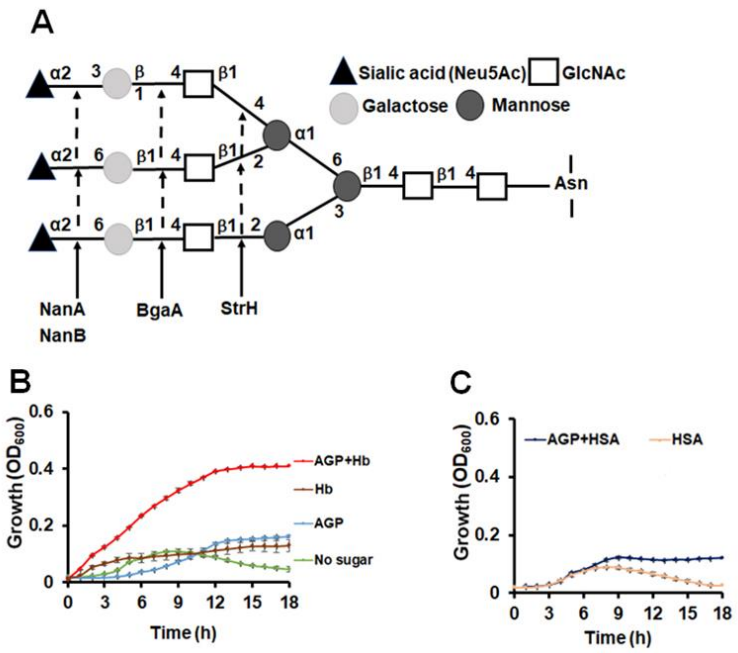

Figure 2.7: Hemoglobin facilitates Spn growth on a human glycoprotein.

(A) Schematic representation of the human α-1-acid glycoprotein (AGP), as described in [22]. Arrows indicate the cleavage sites of the Spn enzymes, neuraminidase (NanA), galactosidase (BgaA), and N-acetylglucosaminidase (StrH). Fresh medium was inoculated with D39 grown on BAPs (18 h, starting $O.D._{600}$ = 0.05). **(B)** Shown is Spn growth in sugar-free CAT medium (no glucose added), or sugar-free CAT with 5 mg/ml AGP, and/or 20 μM hemoglobin (+Hb). **(C)** The same as in (A), only that 20 μM human serum albumin (+HSA) was added instead of hemoglobin. The data are representative of three independent experiments performed in triplicates; error bars indicate SD.

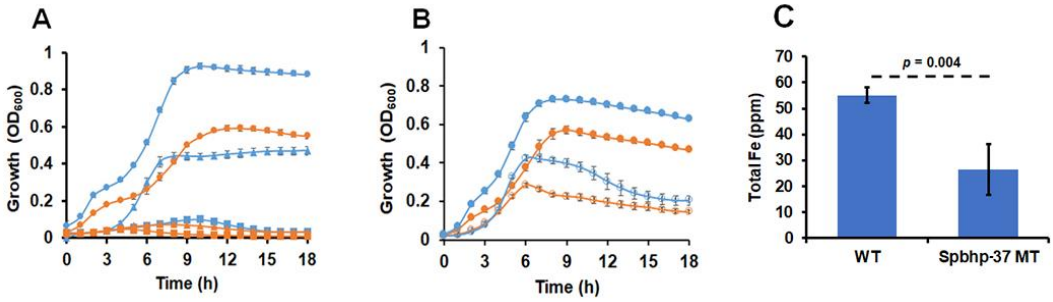

Figure 2.8: The heme/hemoglobin binding protein, Spbhp-37, plays a role in mediating the positive impact of hemoglobin in Spn.

Fresh medium was inoculated with D39 (blue) and the isogenic Δ*spbhp-37* strain (orange) grown on BAPs (18 h, starting $O.D._{600}$ = 0.05). Shown is growth in **(A)** THYB with 3mM di-pyridyl (DP), THYB with DP and 10 µM heme or 20 µM hemoglobin, or **(B)** THYB (empty symbols) or THYB with 20 µM hemoglobin (full symbol). The data are representative of three independent experiments performed in triplicates; error bars indicate SD. **(C)** Total intracellular iron content (ppm) determined by ICP-MS in D39 wild type and Spbhp-37 mutant cultures samples (normalized to optical density) grown in THYB with 20 µM hemoglobin. The data represents the average of three independent biological replicates; error bars indicate SD.

Table 2.1: Strains and plasmids used in this study.

S. pneumoniae	**Description**	**Source or references**
D39	Avery strain, clinical isolate, WT (capsular serotype 2), CSP1	[112], [113]
TIGR4	Invasive clinical isolate, WT (capsular serotype 4), CSP2	[49]
8655	Invasive isolate (serotype 6B), CSP2	CDC
3875	Invasive isolate (serotype 6B), CSP1	CDC
Δ*spbhp-37*	D39-derivative *spbhp-37* null mutant, Ery^r	This study
E. coli		
One shot Top-10	Cloning strain	Invitrogen
Plasmids		
pAF104	Seamless cloning vector pUC19, Amp^r	This study
pCR2.1 TOPO	Cloning vector, Ery^r	[81]

Table 2.2: Primers used in this study.

Target	Primers	Sequence (5′ to 3′)	Comments
pUC19-L	ZE 738-L	TATCAAAGGGCATGCAAGCTTGGCGTAATCAT	cloning
	ZE 739-R	ACTGTGCAGTACCGAGCTCGAATTCACTGGCC	
5′- region of spbhp-37	ZE 740-L	CTCGGTACTGCACAGTAGTAGGTTTCCCTTTG	cloning
	ZE 741-R	TTGTTCATTACTGAACCTCCTAAATAAGATGT	
ermB	ZE 742-L	GTTCAGTAATGAACAAAAATATAAAATATTCT	cloning
	ZE 743-R	CATCAAGGCGACTCATAGAATTATTTCCTCCC	
3′- region of spbhp-37	ZE 744-L	ATGAGTCGCCTTGATGGAAGCGTAAAAGTTCC	cloning
	ZE 745-R	TGCATGCCCTTTGATAGACAAAACCACTTCTT	
aliB	ZE 878-L	GGACTGTTTCTCAGGACGGTTTG	qPCR
	ZE 879-R	CAGCTGCATATTGCAAACCTGTC	
ilvD	ZE 880-L	CCTGGTATGCGTTTCTCTCTAAC	qPCR
	ZE 881-R	AGCAATCATAGATCCAGGCATG	
aliA	ZE 882-L	GGTCACTTATGGGGATGAATGG	qPCR
	ZE 883-R	GGAATGTCACACCTTCTGCTTG	
argG	ZE 884-L	CCTTGGTATCTGCCTTGAGC	qPCR
	ZE 885-R	GATCCAAGGCTGCAATCGATAC	
SPD_1803	ZE 886-L	GGATTGGATGAGGATTTCTACC	qPCR
	ZE 887-R	CTTCTCTAACAAGCCAAGACATG	
gyrB	ZE 661-L	GGCACTGTATGGTATCACACAAG	qPCR
	ZE 662-R	TCTCTAAATTGGGAGCGAATGTC	

Table 2.3: Effect of hemoglobin supplementation on Spn viability.

* NS denotes THYB without supplements, Hb denotes THYB supplemented with 20 μM hemoglobin. Statistical analysis: 8h, *P = 0.02*; 18h, *P = 0.04* (Student t test)

Incubation time (h)	Conditions*	Total (CFU/ml)
8	NS	$2.6 \pm 1.3 \times 10^8$
	Hb	$5.5 \pm 1.1 \times 10^8$
18	NS	$4.7 \pm 3.1 \times 10^2$
	Hb	$8.5 \pm 6.4 \times 10^3$

3 CHAPER II: HEMOGLOBIN INDUCES ROBUST *STREPTOCOCCUS PNEUMONIAE* BIOFILMS VIA THE CSP AND CIARH PATHWAYS: A NEW REGULATORY RIDDLE

Biofilm formation is a crucial stage in the nasopharyngeal establishment and disease progression by the human pathogen *Streptococcus pneumoniae*. *In vitro,* the biofilms pneumococci produce on abiotic surfaces exhibit delayed growth, lower biomass, and lack the structures seen in biofilms grown on epithelial cells or during nasopharyngeal colonization. Herein, we show that the addition of hemoglobin to the medium activates unusually robust and early biofilms in multiple *S. pneumoniae* serotypes grown in batch cultures on abiotic surfaces. Supplementation with denatured hemoglobin, myoglobin, free iron, or heme, did not induce biofilms. Pooled human blood, but not serum, also stimulated biofilms. A mutant in the pore-forming pneumolysin, *ply*, lost the biofilm response to blood but not to hemoglobin. *S. pneumoniae* transitioning from planktonic growth into biofilms in the presence of hemoglobin displayed an extensive transcriptome remodeling. In addition to many changes, we noticed the activation of heme uptake, bacteriocin immunity, and regulatory pathways, including the *ciaRH* and *comCDE* systems. Inactivation of *ciaRH* or *comC* genes resulted in a corresponding reduction of 37% and 67% in biofilm formation respectively. The deletion of *comD* or *comE,* however, had little or no effect on biofilms, respectively. In summary, hemoglobin promotes vigorous pneumococcal biofilms *in vitro*. This response requires the *ciaRH* and *comC* genes. The competence stimulating peptide, CSP-1, functions independently of its cognate two-component system, *comDE*, in promoting biofilms in the presence of hemoglobin. Altogether, these findings provide new and intriguing insights into the interactions between *S. pneumoniae* and its obligate human host.

3.1 Introduction

Streptococcus pneumoniae (Spn) colonizes the nasopharyngeal mucosal surfaces. Asymptomatic carriage facilitates dissemination from person to person and the development of several clinical manifestations, including invasive diseases such as pneumonia, meningitis, and bacteremia. Spn causes 15 million cases of severe infections each year, leading to proximately half a million deaths in children [7, 8]. Resistance to beta-lactams, macrolides, or tetracycline was reported in more than 30% of invasive pneumococcal disease in 2017 [114, 115], leading the World Health Organization to classify Spn in 2017 as one of the top twelve priority pathogens [111, 114, 115].

Spn carriage in the upper respiratory tract and lungs involves the formation of bacterial aggregates developed into biofilms. Pneumococcal biofilms have also been detected in chronic otitis media infection [55] and rhinosinusitis [56]. Local spread and bronchoaspiration may lead Spn to breach the epithelial and endothelial barriers and penetrate tissues, providing access to the bloodstream. Recently, pneumococcal biofilms were described in cardiac microlesions after Spn invasion of the myocardium [57]. Biofilms not only help pneumococci compete with the native flora and serve as reservoirs for pneumococcal spread, but these bacterial structures also assist in the escape from the host immune responses and confer antibiotic resistance [54, 58].

The first *in vitro* model system for pneumococcal biofilm used cellulose Sorbarod filters as the surface, was developed to study antibiotic susceptibility [116]. Since then, several advanced *in vitro* model systems for Spn biofilms were developed by us and others. These biofilm models include static or continuous flow bioreactors with live cultures of respiratory or mucosal epithelial

cells [117-120]. Spn produces pronounced biofilm structures in these tissue culture models [64, 118, 120-122]. Still biofilm formation on abiotic surfaces requires the growth medium to be replenished, logarithmic culture as the inoculum, or the addition of the competence signaling peptide (CSP) to the growth medium. Even with these conditions, pneumococcal biofilms typically develop in batch cultures only after 16-24 hours of incubation [123, 124]. Multiple conditions, such as media type, pH, temperature, and osmolality, influence pneumococcal biofilm formation *in vitro* [54]. Moscoso *et al*., for example, observed robust biofilms in chemically defined or semi-synthetic media, while pneumococci growing in complex media such as CAT or Todd-Hewitt Broth with 5% yeast extract, produced poor biofilms [123].

The role of several bacterial factors in pneumococcal biofilms was established. For example, both sialic acid and choline residues (on the cell-wall teichoic acids) have a positive influence on biofilm development [61]. Hence, inactivation of the neuraminidase *nanA* [119] and several genes encoding choline-binding proteins [123, 125] attenuates biofilms. Capsule production, however, is adversarial to biofilm formation in Spn [125, 126]. Both of the two quorum-sensing systems, Lux and Com, contribute to pneumococcal biofilms [127]. Investigations in model systems, involving abiotic surfaces and human respiratory cells, show that the autoinducer, LuxS (AI-2), is needed in the early stages (24 h post inoculation) of biofilms formation. The *luxS* mutant produced ~80% less biofilm biomass comparing to the wild type strain [120]. The competence stimulating peptide-1 (CSP-1), on the other hand, does not impact the initial attachment of cells to the surface in a microtiter model but promotes stability and maturation of biofilms on abiotic surfaces [124, 128] and in a bioreactor model with human respiratory epithelial cells [120]. The two-component system (TCS) *ciaRH* facilitates pneumococcal stress

response and resistance to antibiotics that target the cell wall. The expression of the response regulator, *ciaR* is induced during biofilm growth [124], and insertion mutants in the histidine kinase, *ciaH*, were isolated by *in vitro* screen for biofilm-attenuated mutants [125, 126]. *In vivo*, the *ciaRH* genes are required for the Spn establishment and biofilm formation in the nasal septa in a murine model [125, 126]. In summary, biofilm development by Spn is multifactorial, and multiple regulatory circuits influence it.

In vivo, biofilms play a vital role in pneumococcal establishment in the upper respiratory tract, ears, lungs, and heart. The host factors that promote the pneumococcal interchange between the planktonic and sessile states are not fully appreciated. We recently discovered that the addition of hemoglobin to the culture medium triggers growth as well as an extensive transcriptome shift that includes many metabolic genes and virulence factors necessary for nasopharyngeal colonization and lung infections (manuscript under review). We, therefore, tested here the hypothesis that hemoglobin also promotes pneumococcal biofilms.

3.2 Materials and Methods

3.2.1 Bacterial strains and growth conditions

The Spn strains used in this study are listed in Table 3.1. Frozen Spn stocks were prepared in the medium Skim milk-Tryptone-Glucose-Glycerin (STGG) as described [77] and kept at -80 °C. Spn STGG stocks were plated on Tryptic Soy blood agar plates (BAPs) and incubated overnight at 37°C under microaerophilic conditions. Spn was also grown in Todd-Hewitt broth containing 0.5% (w/vol) Yeast extract (THYB). One or more of the following supplements were

added to the growth medium as indicated: The iron chelator 2, 2'-Di-pyridyl (Acros organics), bovine hemin (Sigma Aldrich), bovine serum albumin (BSA, Sigma Aldrich), human hemoglobin (Sigma Aldrich), Ferric nitrate nonahydrate ($FeNO_3$, Fisher scientific), equine myoglobin (Mb) (Sigma Aldrich), whole human blood (BioIVT), human serum (Innovative Research), and competence stimulating peptide (CSP1, 200 ng/ml) (Annaspec). The antibiotic erythromycin (ery; 0.5 µg/ml), chloramphenicol (Cm; 4 µg/ml), and tetracycline (tet, 1 µg/ml), was added to the BAP when needed. In some experiments, heat-inactivated hemoglobin (at 99°C for 5 min) and filtered hemoglobin (using Amicon Ultra centrifugal filters, MWCO 10,000), or the flow-through fraction was added to the growth medium.

3.2.2 The growth assays

Fresh medium (with or without supplements) was inoculated with Spn cells collected from BAPs following overnight incubation (starting culture $O.D._{600}$ = 0.05). Cell cultures (200 µl per well) were allowed to grow in 96-well microtiter plates (Coaster 3595, Corning) incubated at 37 ˚C. The culture $O.D._{600}$ was recorded at 1 h intervals for 18 h using (SpectraMax M2 spectrophotometer, Molecular device). For each growth condition, we used wells containing only the medium (and supplements when appropriate) as the blank. Bacterial growth was tested in triplicates.

3.2.3 Biofilm assay on abiotic surfaces

To monitor Spn biofilm formation, an overnight BAP culture (starting culture $O.D._{600}$ = 0.05) was used to inoculate into fresh THYB media (with and without supplement). The culture was grown in microtiter plate for indicated times at 37 ˚C statically. We performed crystal violet

staining to quantitate the biofilm biomass. In brief, the planktonic cultures were removed from the plate and biofilms were washed five times with double-distilled water (ddH_2O) and then allowed to dry for 15 min. Crystal violet (0.1%) was then added, and the biofilms were incubated for 15 min with slow shaking (Lab-Line Maxi Rotator). After washing 4 to 5 times, crystal violet-stained biofilms were allowed to dry at room temperature for 15 min. To quantify biofilm biomass, crystal violet was dissolved by adding 95% ethanol to each well including the blank well and incubated for 15 min at room temperature followed by mixing the suspension by pipetting vigorously. The absorbance at 590 nm of solubilized dye was determined in a SpectraMax M2 spectrophotometer (Molecular device). To determine biofilm cell viability at designated time points, biofilm cells were washed twice with sterile phosphate-buffered saline (PBS) and the plates were sonicated for 15 seconds in a Cole-Parmer ultrasonic cleaner followed by vigorous pipetting to collect all attached bacteria. Biofilm cell counts (CFU/ml) were determined by dilution plating into BAP.

3.2.4 Visualizing Spn biofilm by confocal microscopy

To test the surface specificity for biofilm production, we used an 8-well glass plate as another abiotic surface. An overnight BAP culture of GFP-expressing D39 was used to inoculate the glass plate in a similar method as above. Spn biofilms produced on 8-well glass plate for indicated time points (at 2h, 4h, 6h and 8h) were washed three times with PBS, fixed with 2% paraformaldehyde and stained as previously described [120]. Briefly, the capsules were stained with wheat germ agglutinin conjugated with Alexa Fluor 555 (Molecular Probes, Invitrogen) for 30 min. Nucleic acids were stained with TO-PRO-3 (Molecular Probes) for 15 min. All staining procedures were performed at room temperature. Finally, after washing three times with PBS, the preparations were mounted with Vectashield mounting medium (Vector Laboratories) and

analyzed with a Zeiss LSM 510 confocal microscope. Confocal images were analyzed with LSM Image Browser, version 4.0.2.121.).

3.2.5 Spn growth analysis using human blood and serum ex-vivo

We prepared 0.1%, 0.3%, and 0.5% suspension in sterile phosphate buffered saline (PBS) from whole human blood. Then the suspension was washed three times by centrifuging at 500xg for 5 min at 4˚C in each washing step. Finally, resuspended in fresh THYB media and proceeded with inoculation into microtiter plate with Spn culture using procedures described above. Normal pooled human serum (ranges from 2.5% to 40%) was added to the THYB media followed by filter sterilized the mixture and used in microtiter growth assay. Following overnight growth in a microtiter plate, biofilm formation was assayed using the crystal violet staining method described above.

3.2.6 RNA-Seq analysis

Fresh THYB was inoculated with Spn cells from frozen logarithmic stocks (starting culture $O.D._{600}$ = 0.02), and the cultures were allowed to grow in 12 well microtiter plates (2 ml per well) at 37 °C. 20 µM hemoglobin (in 0.9% saline) or 0.9% saline (negative control) was added to the growing cells at the early logarithmic phase ($O.D._{600}$ = 0.2-0.3). To harvest biofilm samples, planktonic cultures were washed once with sterile 1xPBS (1ml) and added 1ml PBS to each well followed by sonicating the plates for 15 s. Samples of biofilm cultures were collected and processed with RNA protect reagent (Qiagen) following the manufacturer's recommendations and stored the pellet at -80°C until further use. For RNA preparation, cell samples were suspended in

700 µl of Trizol with 300 mg of acid-washed glass beads (Sigma Life Science) and disrupted by vortexing. Total RNA was isolated using the Direct-zol RNA MiniPrep kit (Zymo Research). DNA was removed by the Turbo DNase-free kit (Life Technologies). rRNA was eliminated with the Ribo-Zero Magnetic kit for Gram-positive bacteria (Epicenter). RNA Quality and quantity were assessed using a 2100 Bioanalyzer (Agilent) and NanoDrop 8000 spectrophotometer (Thermo Scientific), respectively.

Directional RNA-Seq libraries were created using the ScriptSeq v2 RNA-Seq Library Preparation kit (Illumina) according to the manufacturer's instructions. A rapid-run 100 bp single-read DNA sequencing was performed at the Institute for Bioscience and Biotechnology Research (IBBR) Sequencing Facility at the University of Maryland, College Park, using the Illumina HiSeq 1500 platform. Data were generated in the standard Sanger FastQ format and raw reads were deposited with the Sequence Read Archive (SRA) at the National Center for Biotechnology Institute. Read quality was evaluated using FastQC software (Babraham Bioinformatics), and mapping against the Spn D39 genome using Bowtie package alignment software [83]. The read count or raw count data for all genes were acquired using Featurecount package [84]. These raw count data files were then used in DESeq2 package [85] to calculate differential expression analysis of all samples for pairwise comparison.

3.2.7 Construction of D39-derived mutant strains

The plasmids used in this study are listed in Table 3.1 and the primers in Table 3.2. To prepare a deletion mutant in *ciaRH*, *yesMN* and *vicK* genes in the background of Spn D39 strain, the mutant alleles containing the *ermC* gene or *cat-194* gene (which confers resistance to

erythromycin, ery^R and chloramphenicol, Cm^R respectively) flanked by the 5' and 3' genomic regions of either *ciaRH* or *yesMN* or the *vicK* genes were prepared using the Gene art seamless cloning kit (Thermo fisher scientific). Briefly, the appropriate genomic segments were amplified from the D39 chromosome using the primer sets indicated in table 3.2. The *ermC* gene, *cat-194* and the pUC19 vector were amplified from pJRS233, pDC123 and pUC19-L plasmids using the primer sets described in table 3.2, respectively. All PCR fragments were purified (using the Minelute PCR purification kit, Qiagen) and cloned into One-shot topo *E. coli* strain, generating plasmid pAF105, pAF106 and pAF108. The resulting allele was then amplified (from pAF105, pAF106 and pAF108) and transformed into competent D39 cells using standard protocols [82]. The mutants were selected on BAPs containing erythromycin (0.5 µg/ml) or chloramphenicol (4 µg/ml). The mutation was confirmed by PCR in the resulting erythromycin-resistant clone (named 2F45 and 2F26) and chloramphenicol-resistant clone (named 2F22) using the primer set ZE 776-L/ZE 781-R, ZE 800-L/ZE 805-R, ZE 784-L/ZE 789-R respectively.

3.3 Results

3.3.1 Hemoglobin induces a rapid formation of Spn biofilms in vitro

We recently observed that the addition of hemoglobin to an iron-deplete medium facilitates vigorous pneumococcal growth that exceeded the one observed in the presence of free iron. Heme also supports Spn growth but is toxic above 10 µM. Notably, we noted growth stimulation also when a standard Todd-Hewitt and yeast extract broth (THYB) was supplemented with hemoglobin but not with free iron or heme (manuscript under review). Here, we examined the impact of additional host heme sources. THYB containing the iron chelator DP was inoculated with Spn

D39, and the cultures were allowed to grow in microtiter plates for 18 h (Fig. 3.1). Pneumococcal did not grow in THYB-DP, but the addition of 20 μM myoglobin or serum (5-40 % V/V) reinstated growth (Fig. 3.1A and data not shown). Growth with myoglobin or serum surpassed the one observed with free iron or heme (Fig. 3.1A). Notably, these heme sources also allowed for better Spn growth in THYB (iron-complete) (Fig. 3.1B). Similar to hemoglobin, Spn cultivation in THYB is stimulated by myoglobin and serum, although not to the same extent as with hemoglobin.

Crystal violates staining (18 h) revealed Spn D39 produced biofilms in the presence of hemoglobin in either standard THYB (Fig. 3.2A) or iron-deplete medium (THYB-DP, Fig. 3.2B). Biofilm induction by hemoglobin occurred in a dose-dependent manner, starting with 0.5 μM hemoglobin in THYB (Fig. 3.2A) or 5 μM in THYB-DP (Fig. 3.2B). We did not observe biofilm formation with myoglobin, heme, or free iron. Similarly, the addition of a control protein (BSA, which has a molecular weight similar to hemoglobin) or denatured hemoglobin did not stimulate biofilm. To exclude the possibility that a contaminant in our hemoglobin preparation was responsible for triggering biofilms, we filtered the hemoglobin solution using 10,000 MW cutoff and tested both fractions. While filtered hemoglobin induced biofilms, the flow-through did not (Fig. 3.2C). Finally, hemoglobin induced biofilms also in six different Spn vaccine strains, including reference strain TIGR4 and EF3030 and clinical isolates (Fig. 3.2D and data not shown). Therefore, biofilm induction is dependent on hemoglobin in its native form and conserved in multiple serotypes.

Following biofilm formation, over time, we found that pneumococci that grew in THYB supplemented with hemoglobin formed significant biofilm biomass as early as 6 hours post-

inoculation and generated most of the biomass within 8 hours of incubation (Fig. 3.3A). In contrast, the controls (THYB) produced little to no biofilms in THYB up to 48 h of incubation. Using viable counts, we found that 3.6-fold more live cells were recovered from the microplate surface in the presence of hemoglobin compared to cultures that grew in THYB alone ($2.2 \pm 0.57 \times 10^8$ Vs. $6.1 \pm 1.94 \times 10^7$ respectively, $P = 0.05$) (Table 3.3). We also used a more sensitive, fluorescent-based method and confocal microscopy to investigate the timing of biofilm formation. The growth of GFP-expressing D39 was visualized by staining the bacterial capsule and DNA. Confocal images (XY optical sections) revealed a rapid formation of biofilms that started at 2 h post-inoculation and plateau at 8 h when D39 was incubated with Hb (Fig. 3.3C).

3.3.2 Human erythrocytes trigger biofilm formation in a Ply-dependent manner

Under physiological conditions, most of the hemoglobin is within the blood erythrocytes. We next examine the impact of supplementing the growth medium with blood. The addition of washed blood cells (0.1 - 0.5%) to THYB triggered robust Spn growth in the two test strains (D39 and TIGR4, data not shown). Biofilm biomass also significantly increased when pneumococci were incubated with blood cells, although to a lower level compared to hemoglobin (Fig. 3.4A). Pneumolysin (Ply) releases hemoglobin from blood cells *in vitro* [129-131]. Hence, we asked if this hemolysin is needed the biofilm response. A *ply* knockout in both D39 and TIGR4 backgrounds did not produce biofilms when grown in THYB supplemented with blood. On the other hand, the *ply* mutants produced robust biofilms in response to hemoglobin (Fig. 3.4B). While the addition of human serum to THYB also enhanced Spn growth (Fig. 3.1B), THYB supplementation with serum (2.5 – 40 %) did not trigger biofilms (Fig. 3.2A, data not shown).

Hence, labile hemoglobin released from erythrocytes by Ply is likely responsible for signaling Spn biofilms.

3.3.3 Spn transitioning to biofilm in the presence of hemoglobin exhibits a significant transcriptome shift

We next examine global gene expression in Spn transitioning into biofilm in the presence of hemoglobin. Hemoglobin or saline (as a control) was added to Spn cultures grown in THYB at the early log phase, and culture samples were collected one- and two-hours post-treatment. RNA was isolated from four biological replicates for each growth condition and analyzed by RNA-Seq. The global transcriptome in planktonic Spn was compared to that in sessile cells (recovered from the microtiter surface). Note that Spn did not produce biofilms when grown in THYB under our experimental conditions; hence we could not compare gene expression among biofilm cells growth with and without hemoglobin. The comparison between planktonic and early biofilms cells (both with hemoglobin, two biological replicates) revealed a significant transcriptome shift that took place mostly within the first hour after hemoglobin addition. 322 and 136 genes were correspondently up- and down-regulated in the first hour after treatment (Fig. 3.5A & B). To adjust to biofilm growth, Spn differently expresses metabolic pathways and reduces the expression of genes involved in translation and transcription [132]. We observed a similar response during growth in early biofilms in the presence of hemoglobin (Fig. 2.6). For example, many PTS systems and other genes related to carbohydrate metabolism were repressed in sessile cells in the presence of hemoglobin. These include the *bgu* (SPD_1830-33) and *lacABCD* (SPD_1050-54) operons.

The transition from planktonic growth to biofilms in the presence of hemoglobin was associated with the induction of several genes whose expression is induced during infection and are vital for biofilm formation *in vivo* (Fig. 3.6A). These genes include *nanA*, neuraminidase that catalyzes the release of terminal sialic acid residues from the host glycoconjugates. The transcription of the *nanA* genes is activated during lung infection, and this enzyme is essential for Spn biofilm formation in the nasopharynx [62]. Compared to planktonic cells, Spn in early biofilm exhibited higher expression of the heme importer, *piuBCDA*, and the operon encoding *spbhb22*, which is implicated in heme uptake [53] (SPD_1590, Fig. 3.6A). The ferrochrome-binding protein, *piaA*, was, on the other hand, repressed in the surface attached cells (Fig. 3.6B).

The transition from planktonic growth to biofilms in the presence of hemoglobin was associated with the induction of quorum sensing systems, two-component systems (TCS), and putative regulators. For example, the signaling peptide, *phrA* was activated together with the associated lantibiotic-synthesis gene cluster encoded by the Region of Diversity 12 (RD12 [133, 134], Fig. 3.6A). Notably, the TrpA/PhrA-controlled gene cluster is not expressed *in vitro* (in regular laboratory medium), but its transcription is activated during heart infection [57]. The lantibiotic-immunity genes, *blpYZ* were also induced in biofilm-forming pneumococci, as well as several genes from the *com* regulon (i.e., *comCDE*, *comAB*, *amiEDCA*, *cbpD*, and *cinA*). In addition to *comDE*, the two-component systems (TCSs) *yesMN*, *ciaRH*, *vicRK* and *liaSR*, were also induced (Fig. 3.6A), reflecting the complexity of the biofilm response to hemoglobin.

3.3.4 Biofilm formation in the presence of hemoglobin require comC and ciaRH genes

To test for a possible role in the biofilm response to hemoglobin, we tested mutants in regulatory genes that were up regulated in pneumococci that are transitioning into biofilms in the

presence of hemoglobin. Deletion mutant in *comC* (encoding CSP-1 peptide), and TCS *ciaRH*, *yesMN*, and in the histidine kinase *vicK* (vicR is an essential gene) were examined in biofilm production (Fig. 3.7). All the tested mutants produce significant biofilms when grown in the presence of hemoglobin compared to growth in standard THYB (18 h, Fig. 3.7A). No significant difference in biofilm biomass generated by the Δ*yesMN* and Δ*vicK* mutants compared to the parental D39 strain when grown in THYB with hemoglobin (Fig. 3.7A). Inactivation of *ciaRH* or *comC*, however, resulted in 37% (P = 0.01) and 67% (P = 0.001) reduction in biofilm biomass, respectively. Since the inactivation of *comC* was the most detrimental for biofilms development in our experimental conditions, we also tested individual deletions in the histidine kinase *comD* and the response regulator, *comE,* which mediates CSP-1 signaling. Surprisingly, the deletion of *comD* resulted in a 20% (P = 0.04) reduction in biofilm production, while the deletion of *comE* had no impact (Fig. 3.7B). Supplementing the medium with CSP-1, corrected the phenotype observed with the Δ*comC* and Δ*comD* strains, but had no significant influence on biofilm production by the *comE* or *ciaRH* mutants. Together, the data demonstrate that both *comC* and *ciaRH* genes are involved in biofilm production in the presence of hemoglobin and that *comC* orchestrate the response almost completely independently of *comDE*.

3.4 Discussion

Environment sensing is essential to the transition of biofilm-forming microbes from a planktonic to a sessile state. The corresponding transcriptome adjustment guides the global physiological and metabolic changes that take place during biofilm development, from the initial attachment up to biofilm maturation. Spn is a colonizer of the upper respiratory tract, who is well adapted to its obligate human host. The host factors that play a role in biofilm formation during

colonization in Spn are not fully appreciated [3, 15, 17, 54, 127]. Our group recently discovered that the addition of hemoglobin to the medium activates the expression of many pneumococcal genes with an established role in colonization. Here, the data show that hemoglobin induces early and robust pneumococcal biofilm structures that are typically not observed in abiotic models *in vitro*. Spn transitioning into biofilms with hemoglobin exhibit an extensive transcriptome shift, activating genes that are typically expressed *in vivo* during biofilm growth. The pneumococcal biofilm response to hemoglobin is mediated by a new mechanism that involves the *comC* and *ciaRH* genes. Below we discuss these intriguing observations and the implication on the current understanding of pneumococcal physiology and virulence.

Spn biofilms formed on abiotic surfaces typically exhibit a delayed growth and lower biomass compared with biofilms growth on epithelial cells or in the nasopharynx *in vivo* [118, 119, 135]. Moreover, non-encapsulated strains produce more biofilm than encapsulated strains [123, 125]. Surprisingly, the addition of hemoglobin to THYB, as the sole iron source or as a supplement, triggered a dose-depended biofilm formation in several encapsulated strains, including vaccine serotypes (Fig. 3.2D). In the presence of hemoglobin, biofilm development was unusually early (within 2 - 8 h of incubation) compared to typical *in vitro* models (which takes 18-24 h [127]) and vigorous leading to considerable biomass and structures (Fig. 3.3).

Ferric iron (~50 μM) induced a significant increase of Spn biofilms in C+Y medium [136]. Under our experimental conditions, iron did not influence biofilm formation, perhaps because of the different growth conditions (THYB vs. C+Y). Likewise, the addition of free heme, myoglobin, or serum had no impact on biofilm formation (Fig. 3.2A & B), supporting the notion that

hemoglobin induction of biofilms is not solely due to the ability of hemoglobin to donate iron or heme. Moreover, myoglobin and serum did not induce biofilms, although they promoted more vigorous growth in THYB and THYB-DP (Fig. 3.1). These observations suggest that the influence of hemoglobin on pneumococcal growth (which might be related to the heme it carries) is separated from its impact on biofilm formation.

Supplementation with a control protein (BSA) or the flow-through after hemoglobin filtration did not promote biofilms (Fig. 3.2C), showing that biofilm signaling is not triggered by non-specific addition of peptides or the presence of possible contaminants. Heat inactivation diminished hemoglobin activation of biofilms. While serum did not induce biofilms, washed blood cells promoted pneumococcal biofilms in wildtype Spn but not in a *ply* mutant (Fig. 3.4A), the mutant, however, produced biofilms in response to the presence of hemoglobin (Fig. 3.4B). Therefore, its labile hemoglobin released from erythrocytes by Ply that is inducing biofilms in the presence of blood. Together, the data show that hemoglobin, in its native form, signals biofilm formation in Spn by an unknown mechanism. The data also imply that the biofilm response to hemoglobin can take place *in vivo* when Spn encounters blood.

In general, we found that the transcriptome of Spn cells transitioning into biofilms in the presence of hemoglobin had the hallmarks of a typical transcriptome of pneumococcal cells during biofilm growth [124] (Fig. 3.6). Few noteworthy examples of Spn gene expression pattern during biofilm growth are virulence gene, *nanA* and regulators, *comE, ciaR*, and *mgrA* [124]. Remarkably, among the highly transcribed genes under our growth conditions, we found the virulent determinants (from the core pneumococcal genome) that are strongly expressed by Spn when

grown in biofilm in the heart. These include *spxB* (pyruvate oxidase), *pspA* (pneumococcal surface protein A), *pavB* (pneumococcal adhesion and virulence protein B), *zmpB* (zinc metalloprotease B), *lytA* (autolysin), *ply* (pneumolysin), and *pcpA* (pneumococcal choline-binding protein A). The *spx* gene, whose expression was amongst the highest, is needed for Spn biofilm formation both *in vivo* and *in vitro*, possibly by driving the formation of biofilm required products [126, 137].

Transcriptome studies revealed the induction of several regulatory systems in early biofilms cells, hence, implicating them in the biofilm response to hemoglobin (Fig. 3.6A). The mutant analysis demonstrated a role only for *comC* and *ciaRH* genes (Fig 3.7). These findings are consistent with the part in biofilm development reported previously for both regulatory circuits [124-126, 128]. The *comC* gene orchestrates competence development in Spn by activating the ComD histidine kinase, which relays the signal to the ComE response regulator, which in turn activates the *com* regulon (including the *comCDE* operon [138]). The data show that inactivation of *comC* resulted in the biggest loss of biofilm formation in Spn grown with hemoglobin (Fig. 3.7A), and this phenotype was complemented by the external addition of CSP-1. Interestingly, CSP-1 functions in biofilm development in the presence of hemoglobin is mostly independent of the *comDE* pathway (Fig. 3.7B), suggesting the presence of a new signaling route for CSP-1 [139].

The CiaRH mutant exhibited a significant reduction in biofilm formation as well (Fig. 3.7A), and the addition of CSP-1 did not compensate for the loss of *ciaRH*, suggesting the two systems likely operate independently of each other. The CiaRH TCS orchestrates the integrity retention of the pneumococcal cell wall by preventing the lysis that is otherwise induced by stress, antibiotic treatment, or competence development [140-143]. Interestingly, Spn senses free sialic acid and upregulates *ciaR* in that sensing response. CiaR, in turn, indirectly regulates the activation

of the *nanAB* genes, which respectively code for sialic acid cleavage (from the host glycoconjugates) and uptake [144, 145]. Free sialic acid act as a signal for pneumococcal biofilms *in vitro* and *in vivo* during colonization of the nasopharynx and lungs in a mouse carriage model [61]. It is not clear, however, how CiaRH contributes to biofilm development in the presence of hemoglobin. The significant biofilm formation exhibited by the *comC* and *ciaRH* mutants (Fig. 3.7A) demonstrates a redundancy in the pathways that orchestrate the biofilm response by hemoglobin. We speculate that hemoglobin signaling of biofilms takes place from the pneumococcal surface since hemoglobin is too big to diffuse through the cell wall and enter the cell. A surface receptor and/or a hemoglobin-dependent heme importer might be needed to rely on the signal, which leads to activation of the *ciaRH* and the *comCDE* genes. CSP-1 generation then promotes signaling *via* unknown regulatory protein.

To our knowledge, this study is the first to present a biofilm induction by hemoglobin in the genus *Streptococcus*. Other streptococci of the oral cavity share orthologs of the *com* and *cia* system speculating if hemoglobin biofilm is a phenomenon found in these systems [146-149]. Recently, a study has reported that hemoglobin also induces biofilms in *Staphylococcus aureus*, and increased colonization was observed in patients with frequent nose bleeds [150]. Collectively, the observation of hemoglobin biofilm induction may help bridge the gap of understanding the biofilm lifecycle of pneumococcus and other biofilm bacteria *in vivo*.

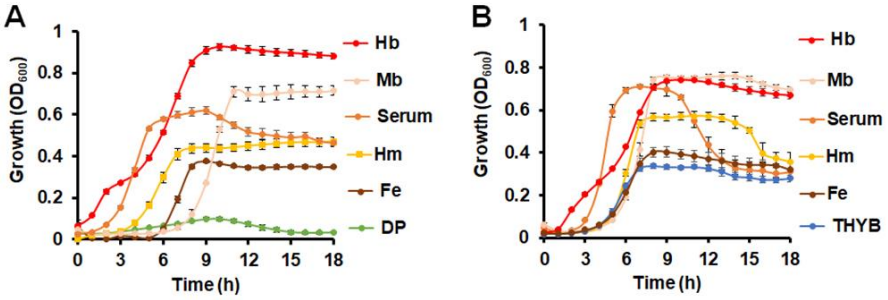

Figure 3.1: Myoglobin and serum promotes pneumococcal growth in iron deplete and iron complete THYB.

THYB was inoculated with D39 cells grown on BAPs (18 h, starting $O.D._{600}$ = 0.05). Shown is growth in **(A)** THYB with 3mM di-pyridyl (DP), THYB with DP and 2 mM of $FeNO_3$ (Fe), 10 µM Heme (Hm), 10% human serum (serum), 20 µM equine myoglobin (Mb), or 20 µM hemoglobin (Hb); **(B)** THYB, THYB supplemented 2 mM of $FeNO_3$ (Fe), 10 µM Heme (Hm), 10% human serum (serum), 20 µM equine myoglobin (Mb), or 20 µM hemoglobin (Hb). The data are representative of three independent experiments performed in triplicates; error bars indicate SD.

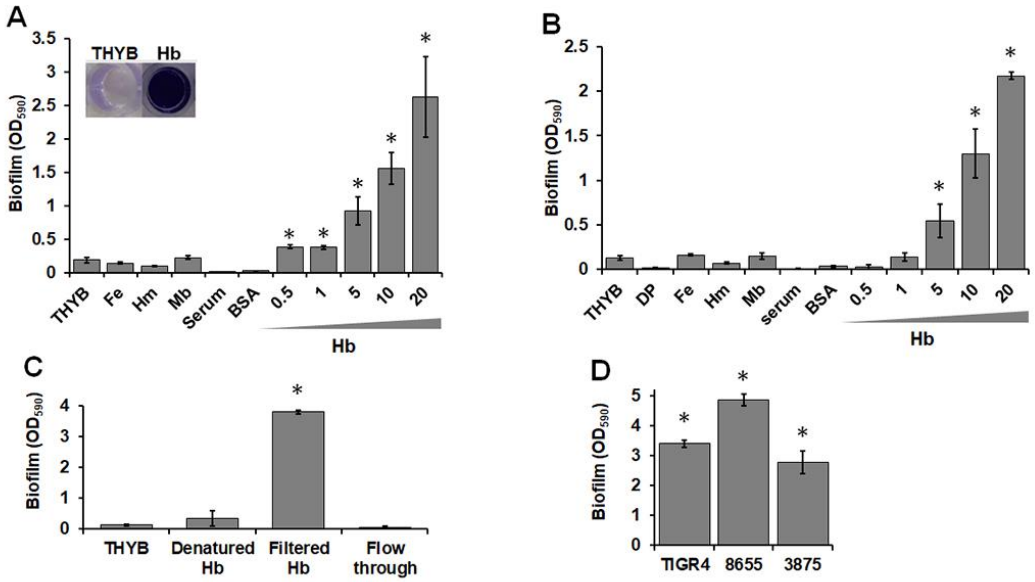

Figure 3.2: Hemoglobin enhances pneumococcal biofilm formation.

THYB was inoculated with Spn cells grown on BAPs (18 h, starting O.D.$_{600}$ = 0.05). Cultures were allowed to grow in microtiter plates, biofilm was quantified (18 h). Shown is D39 grown in (**A)** THYB, THYB with 80µM $FeNO_3$ (Fe), 10 µM Heme (Hm), 20 µM equine myoglobin (Mb), 10% human serum (serum), 20 µM BSA (BSA), or 0.5 to 20 µM hemoglobin (Hb); (**B)** THYB with 3mM DP (DP), THYB with DP and 2mM $FeNO_3$ (Fe), 20 µM BSA (BSA), 10 µM Heme (Hm), 20 µM equine myoglobin (Mb), 10% human serum (serum), 20 µM BSA (BSA), or 0.5-20 µM hemoglobin (Hb); and (**C)** THYB with 20 µM denatured hemoglobin, filtered hemoglobin, or the flow-through after hemoglobin filtration. (**D)** Growth of TIGR4 and the clinical isolates 8655 and 3875 in THYB with 20 µM Hb. Insert shows crystal violet staining following growth in THYB with or without hemoglobin (18 hours). The data are expressed as the mean ±

SD of at least two independent experiments each done in triplicates. The asterisks denote statistically significant difference, P ≤ 0.05 (THYB-Hb vs. THYB in A-D, Student's t-test).

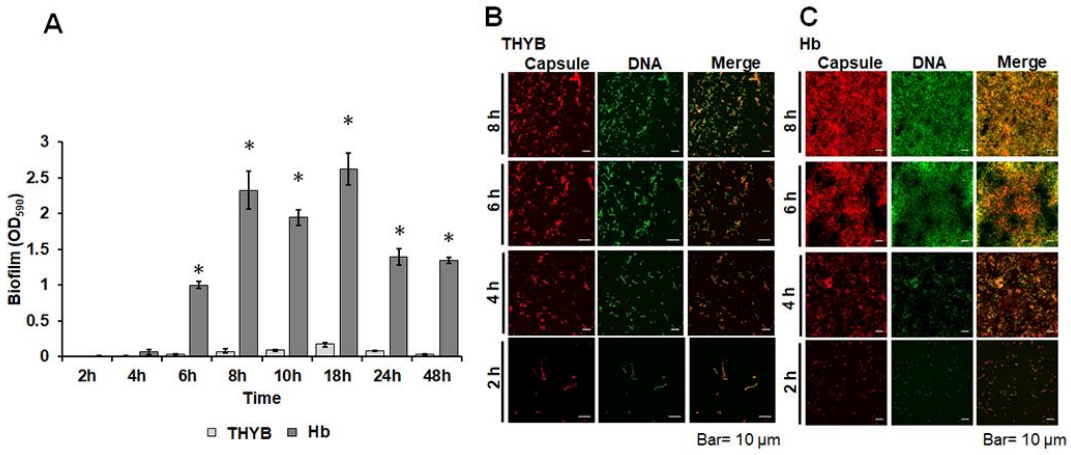

Figure 3.3: Hemoglobin induces early and robust biofilm structures.

THYB with 20 µM hemoglobin (Hb) was inoculated with D39 grown on BAPs (18 h, starting $O.D._{600}$ = 0.05). (**A**) Cultures were allowed to grow in microtiter plates, biofilm and biomass were quantified different time points. The data are expressed as the mean ± SD of at least two independent experiments each done in triplicates. The asterisks denote statistically significant difference, P ≤ 0.05 (THYB-Hb vs. THYB, Student's t-test). Confocal micrographs of biofilms produced by GFP-expressing D39 [81] grown in 8-well glass wells in (**B)** THYB or in (**C)** THYB with 20 µM hemoglobin. The DNA stained with TO-PRO-3 (green) and the capsule with Alexa Fluor 555-labeled anti-serotype specific antibodies (red).

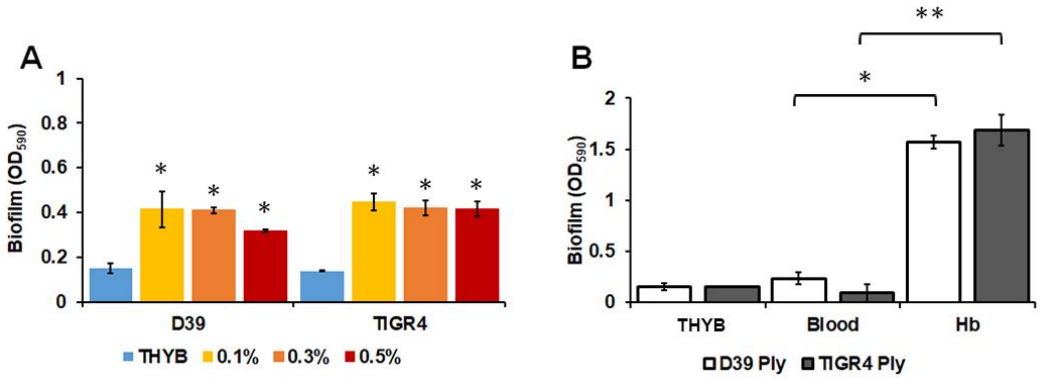

Figure 3.4: Blood cells activates biofilm formation in a ply-dependent manner.

THYB was inoculated with Spn cells grown on BAPs (18 h, starting $O.D._{600}$ = 0.05). Cultures were allowed to grow in microtiter plates. Shown is biofilm formation (18 hours) by **(A)** D39 and TIGR4 grown in THYB or THYB supplemented with 0.1 - 0.5 % (v/v) washed blood cells; **(B)** Δ*ply* mutants in D39 and TIGR4 (filled) background grown in THYB, THYB and 0.3% washed human blood cells (blood), or 20 µM hemoglobin (Hb). The data are expressed as the mean ± SD of at least two independent experiments each done in triplicates. The asterisks denote statistical significance, $P \leq 0.05$ (THYB vs. THYB-blood, in A and THYB-blood vs. THYB-Hb in B, Student's t-test).

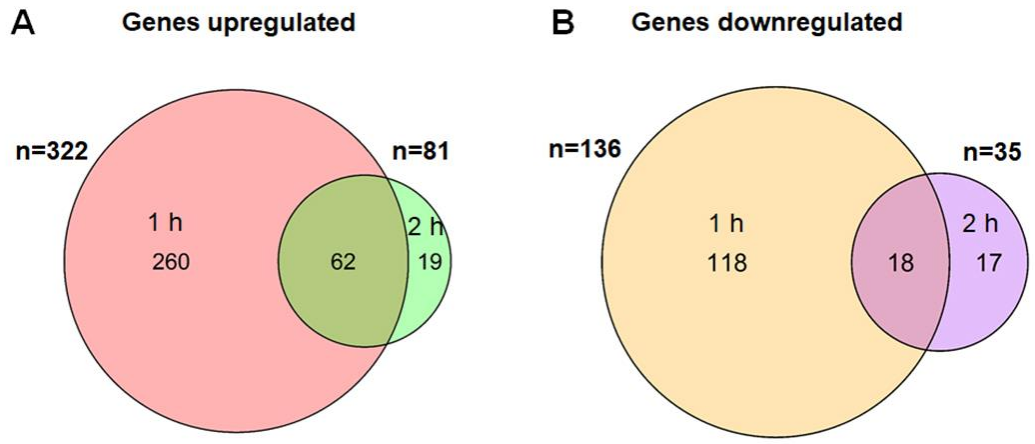

Figure 3.5: Spn transition from planktonic to biofilm growth in the presence of hemoglobin involves transcriptome remodeling.

Venn diagram (using R**)** of differentially expressed genes in hemoglobin biofilm cells compared to hemoglobin planktonic cells (fold change ≥ 2). **(A)** Genes upregulated; **(B)** Genes downregulated.

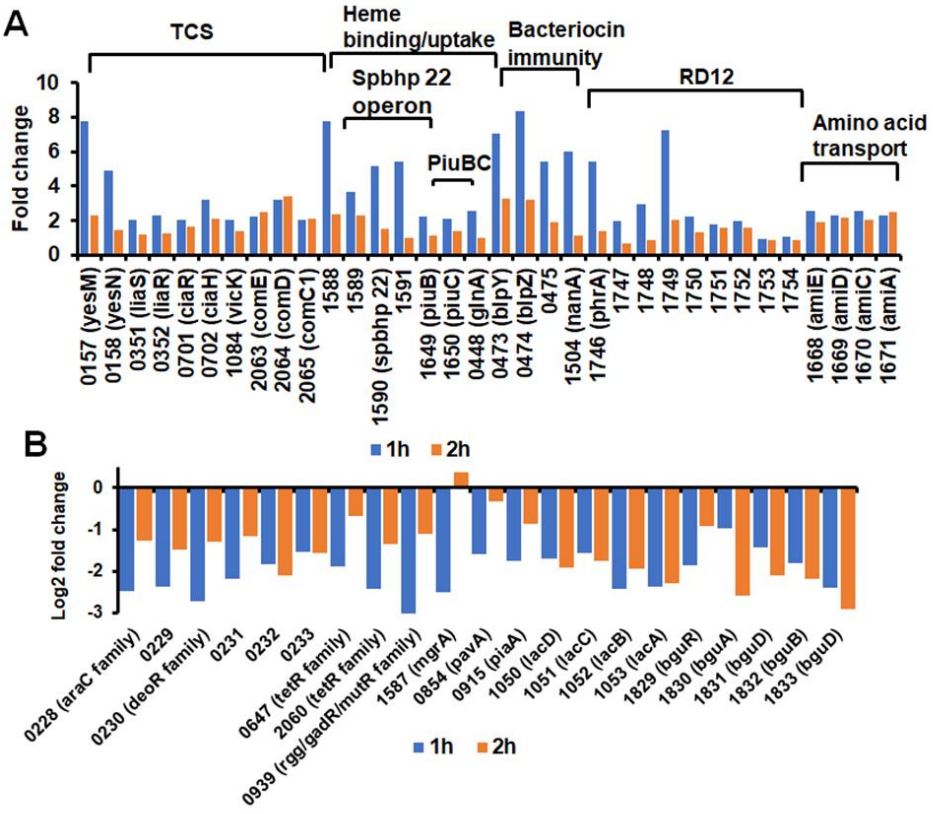

Figure 3.6: Differential gene expression in Spn grown in early biofilm.

The relative expression of selected genes in biofilms vs. planktonic cells (both with hemoglobin) at 1 h and 2 h post hemoglobin addition (Y-axis) is plotted for D39 genes (X-axis). **(A)** up-regulated genes. **(B)** down-regulated genes.

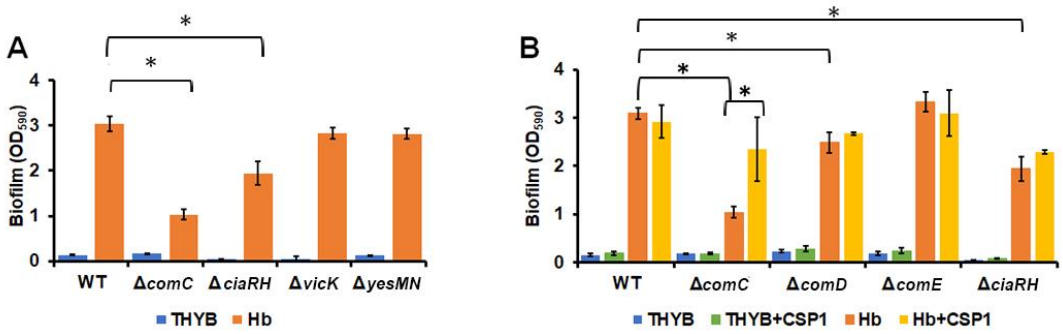

Figure 3.7: Hemoglobin signaling of biofilms involves the comC and ciaRH genes.

THYB was inoculated with Spn cells grown on BAPs (18 h, starting O.D.$_{600}$ = 0.05). Cultures were allowed to grow in microtiter plates; biofilm was quantified (18 h). Shown is biofilm biomass produced by D39 and isogenic mutants were grown in (**A)** THYB or THYB with 20 μM hemoglobin (Hb); and (**B)** in THYB with Hb and CSP1 (200 ng). The data are expressed as the mean ± SD of at least two independent experiments each done in triplicates. The asterisks denote statistical significance, $P \leq 0.05$ (wild-type vs. mutant in the presence of Hb or Hb+CSP1, Student's t-test).

Table 3.1: Strains and plasmids used in this study.

Strains	**description**	**Source or references**
***S. pneumoniae* strains**		
D39	Avery strain, clinical isolate, WT (capsular serotype 2), CSP1	[112], [113]
D39 (SPJV01)	GFP-expressing strain, D39/pMV158GFP Tet^r	[81]
TIGR4	Invasive clinical isolate, WT (capsular serotype 4), CSP2	[49]
8655	Invasive isolate (serotype 6B), CSP2	CDC
3875	Invasive isolate (serotype 6B), CSP1	CDC
Δ*ply* (SPJV14)	D39-derivative *ply* null mutant, Ery^r	[151]
Δ*ply* (SPJV18)	TIGR4-derivative *ply* null mutant, Ery^r	
Δ*luxS* (SPJV05)	D39-derivative *luxS*-null mutant, Ery^r	[81]
Δ*comC* (SPJV10)	D39-derivative *com*C null mutant, Ery^r	[120]
Δ*comD* (SPJV31)	D39-derivative *com*D null mutant, Cm^r	
Δ*comE* (SPJV32)	D39-derivative *com*E null mutant, Cm^r	
Δ*ciaRH* (2F45)	D39-derivative *ciaRH* null mutant, Ery^r	This study
Δ*yesMN* (2F26)	D39-derivative *yesMN* null mutant, Ery^r	This study
Δ*vicK* (2F22)	D39-derivative *vicK* null mutant, Cm^r	This study
***E. coli* strains**		
One shot Top-10	Cloning host containing pJRS233 or pDC123	This study
Plasmids		
pMV158GFP	*S. pneumoniae* mobilizable plasmid containing the green fluorescent protein gene	[152]
pJRS233	Temperature sensitive vector containing *ermC*, Ery^r	This study
pDC123	Vector containing *cat-194*, Cm^r	This study
pAF105	Seamless cloning vector pUC19 for *ciaRH* deletion, Amp^r	This study
pAF108	Seamless cloning vector pUC19 for *yesMN* deletion, Amp^r	This study
pAF106	Seamless cloning vector pUC19 for *vicK* deletion, Amp^r	This study

Table 3.2: Primers used in this study.

Target	Primers	Sequence (5' to 3')	Comments
pUC19-L	ZE 774- L	TGATTCTCGGCATGCAAGCTTGGCGTAATCAT	*ciaRH*
	ZE 775-R	TAAGACTCGTACCGAGCTCGAATTCACTGGCC	cloning
5'- region of ciaRH	ZE 776-L	CTCGGTACGAGTCTTATCTGGTGGTTTCAGCT	*ciaRH*
	ZE 777-R	CACACGGTCATGAGAAACTCCTCCTTATTAAA	cloning
ermC	ZE 778-L	TTCTCATGACCGTGTGCTCTACGACCAAAACT	*ciaRH*
	ZE 779-R	GCATTATCCCGTGGAATTCCCCCCTTAACTTA	cloning
3'- region of ciaRH	ZE 780-L	TTCCACGGGATAATGCCGTCAAGTATACTGAG	*ciaRH*
	ZE 781-R	TGCATGCCGAGAATCATGCCCGTAAGAAAATT	cloning
pUC19-L	ZE 798-L	ATGTTTTGGGCATGCAAGCTTGGCGTAATCAT	*yesMN*
	ZE 799-R	CTTGAGACGTACCGAGCTCGAATTCACTGGCC	cloning
5'- region of yesMN	ZE 800-L	CTCGGTACGTCTCAAGCAACCTGATTTTCTAT	*yesMN*
	ZE 801-R	CACACGGTATCATTTCGAACATAGAGGTCATC	cloning
ermC	ZE 802-L	GAAATGATACCGTGTGCTCTACGACCAAAACT	*yesMN*
	ZE 803-R	TATTGACCCCGTGGAATTCCCCCCTTAACTTA	cloning
3'- region of yesMN	ZE 804-L	TTCCACGGGGTCAATACCGTATGAATGAAAAT	*yesMN*
	ZE 805-R	TGCATGCCCAAAACATAGCCAACGTAAGTATA	cloning
pUC19-L	ZE 782-L	AGAAAGAAGGCATGCAAGCTTGGCGTAATCAT	*VicK*
	ZE 783-R	CACAATAGGTACCGAGCTCGAATTCACTGGCC	cloning
5'- region of vicK	ZE 784-L	CTCGGTACCTATTGTGTCTTCTGACTATTTTT	*vicK*
	ZE 785-R	CATCGGTCTCAAGCATTATTTCTCATGTAATA	cloning
Cat-194	ZE 786-L	ATGCTTGAGACCGATGATGAAGAAAAGAATTT	*vicK*
	ZE 787-R	TCACTCTTTTATAAAAGCCAGTCATTAGGCCT	cloning
3'- region of vicK	ZE 788-L	TTTTATAAAAGAGTGAATACGGCAAGGGTTCA	*vicK*
	ZE789-R	TGCATGCCTTCTTTCTATATCTCTGTCAATGG	cloning

Table 3.3: Biofilm cell counts.

*NS denotes THYB, Student t test statistical analysis, 6h (P=0.05), 8h (P=0.05)

Incubation time (h)	Conditions	Biofilm (CFU/ml)
6	NS	$6.1 \pm 1.94 \times 10^7$
	Hb	$2.2 \pm 0.57 \times 10^8$
8	NS	$4.27 \pm 2.6 \times 10^7$
	Hb	$1.61 \pm 0.41 \times 10^8$

4 GENERAL DISCUSSION

Spn requires iron for growth and obtaining the metal from the host heme and hemoproteins is crucial for the host persistence and establishment of infection. During infections, heme bound to hemoglobin serves as a significant reserve for metal iron; yet substantial knowledge gaps exist concerning the role of heme and hemoglobin as nutrients in Spn physiology and infection. This dissertation addressed these important knowledge gaps and examined the role of hemoglobin as a nutrient and described the part of this host protein in pneumococcal adaptation to the host environment. The data showed that hemoglobin is a preferred iron source and suggest that heme metabolism benefit Spn growth. The experiments demonstrated that hemoglobin promotes Spn biofilms and has a dramatic impact on the bacterial transcriptome. These new observations and their impact on the current understanding of Spn interactions with its human host are discussed below.

The fermentative anaerobe, Spn, is quite fastidious and difficult to cultivate under laboratory conditions. One of the main observations made in this study is that hemoglobin induces a robust Spn growth *in vitro* and shapes Spn transcriptome (Chapter one). The hemoglobin-dependent growth stimulation is observed in both iron-deplete or complete medium independently of the growth assay and is conserved in multiple strains. Spn typically exhibits limited growth in batch cultures and enters early into the stationary phase. The reason for the limited growth Spn exhibits *in vitro* is not fully understood. Acidification and other growth conditions were suggested to limit cultivation. Controlling for these and other factors, however, did not improve Spn cultivation uniformly [65, 105]. The data in Chapter one show that hemoglobin expands Spn growth in a medium that was not otherwise replenished, without pH control, with or without pre-cultivation. The possibility that the positive growth impact of hemoglobin results from an intrinsic

peroxidase activity [88], and thus defense from hydrogen peroxide [89], was ruled out. Moreover, the data show that hemoglobin in its native form provides Spn with growth advantage rather than a nonspecific increase in peptides and amino acids availability, or the presence of low molecular weight contaminants. Together, these observations raise the novel hypothesis that hemoglobin redirects a regulatory mechanism(s) that otherwise leads to premature growth arrest during *in vitro* cultivation by a novel mechanism. In addition to this novelty, the identification of hemoglobin as a Spn growth factor has important implications, since methods to optimize and improve pneumococcal growth are needed to achieve maximum biomass (and capsular production) for vaccine preparations.

The role of iron hemostasis in hemoglobin growth promotion is somewhat puzzling. Growth with hemoglobin did not lead to an elevated level of cellular iron, suggesting that hemoglobin does not supply Spn with the iron it needs to reach its maximal growth potential. Moreover, Spn cells grown in THYB supplemented with ferric iron imports less of the metal compared to cells grown in THYB or THYB with hemoglobin. These observations support a new premise that heme is more useful for the pathogen's physiology then free iron, and therefore, by donating heme, hemoglobin provides Spn with a highly beneficial growth nutrient. Mutant analysis established the role of Spbhp-37 in the acquisition of iron from heme or hemoglobin. Inactivation of *spbhp-37* also impaired Spn growth even in standard THYB, suggesting that heme is the key iron source for Spn in THYB. These findings provided additional support to the idea stated above that heme is growth advantageous for Spn. The reduced growth of the mutant even in the presence of hemoglobin in THYB compared to the wildtype suggest that this hemoglobin receptor mediate, at least in part, the growth benefits of hemoglobin.

Hemoglobin has a significant impact on Spn transcriptome. Most noteworthy changes in this transcriptome shift included changes in the expression of metabolic and virulence genes with an established role in colonization. Furthermore, hemoglobin induces the expression of genes involved in the uptake and use of host-derived sugars found in the mucosa and extracellular matrix. Together with *in vitro* growth experiments, the data show that the presence of hemoglobin is an essential cue for Spn and implies that hemoglobin promotes pneumococcal adaptation to the respiratory tract and mucosal surface. The proposal that hemoglobin served not only as an iron source but also activates host adaptation is a novel concept in the area of host-pathogen interactions, which merit additional inquiries into the mechanism involved.

Another significant finding of this project is the observation that hemoglobin induces early and robust pneumococcal biofilm structures *in vitro* (Chapter two). Pneumococcal biofilms are observed *in vivo* in multiple sites and different stages of infection, while the pathogen exhibits only limited biofilm growth and structures *in vitro.* These perplexing characteristics of Spn suggest that *in vitro* model systems are missing an essential element of true infection. Hence, the finding that the simple addition of hemoglobin to the growth medium is sufficient to induce vigorous biofilm growth is exciting and supports the hypothesis that the hemoglobin signals the host environment to Spn.

The addition of hemoglobin to THYB, either as the sole iron source or as a supplement, triggered a dose-depended biofilm formation in several encapsulated strains, including vaccine serotypes. This biofilm response is dependent on hemoglobin and is not seen with other host proteins, heme or iron, but was conserved in multiple serotypes. While the addition of myoglobin and serum promotes more robust pneumococcal growth, these host heme sources did not induce

biofilms. These observations provide new insights into the pneumococcal response to hemoglobin; First, if growth promotion is associated with host heme sources and not just with hemoglobin, it suggests that it's the heme in hemoglobin, myoglobin, and serum benefits Spn physiology. Free heme does not have this effect, likely due to toxicity. Furthermore, the finding that only hemoglobin promotes biofilm development indicates that separate mechanisms mediate the growth and biofilm response to hemoglobin in Spn. *Ex-vivo* experiments showed that washed blood cells supported biofilms in a Ply dependent manner. These observations suggest that Ply releases the hemoglobin from the erythrocytes, which in turn activates biofilms. These data also imply that the biofilm response to hemoglobin can take place *in vivo* when Spn encounters blood.

Transcriptome analysis shows that Spn transitioning into biofilms with hemoglobin exhibit a widespread shift, activating genes that are expressed *in vivo* during biofilm growth [124, 153]. These studies revealed the induction of several two-component regulatory systems in early biofilms cells. The mutant analysis led to the conclusion that the pneumococcal biofilm response to hemoglobin is mediated by a new mechanism (see proposed biofilm model) that involves the *comC* and *ciaRH* genes. While the findings are consistent with the part in biofilm development reported for both the *comCDE* and *ciaRH* systems [124-126, 128], the discoveries also expose the existence of a new regulatory element(s). Specifically, inactivation of *comC* resulted in the most significant loss of biofilm formation in Spn grown with hemoglobin, while the loss of *comD* or *comE* had only limited influence. Therefore, for biofilm development in the presence of hemoglobin, CSP-1 functions mostly independent of the *comDE* pathway [139]. The biofilm formation still exhibited by the *comC* and the *ciaRH* mutants show that there is a redundancy in the channels that orchestrate the biofilm response by hemoglobin. We speculate that hemoglobin

signaling of biofilms takes place from the pneumococcal surface since hemoglobin is too big to diffuse through the cell wall and enter the cell. A surface receptor and or a hemoglobin-dependent heme importer are likely to be needed to rely on the signal that leads to activation of the *ciaRH* and the *comCDE* genes (see proposed biofilm model).

Biofilms play a crucial role in pneumococcal establishment in the nasopharynx, ears, lungs, and heart *in vivo*. However, the biofilm regulatory network has not been entirely elucidated. The new observation of Spn biofilm induction by hemoglobin promotes the current understanding of the biofilm lifecycle in Spn and possibly other biofilm bacteria. More work is needed to identify the signaling partner(s) for CSP-1 to activate biofilms in the presence of hemoglobin and the mechanism that mediates the part of CiaRH.

In summary, this dissertation informs current paradigms in pneumococcal physiology and virulence. It expands the role of hemoglobin from a nutrient into a key player in Spn interactions with its human host.

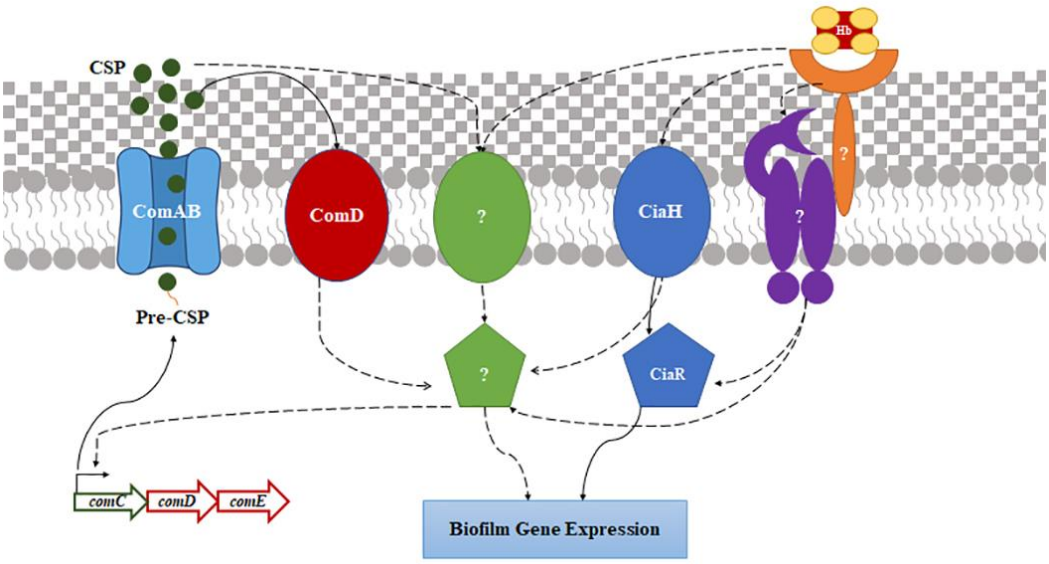

Figure 3.8: Proposed model for biofilm induction by hemoglobin.

Hemoglobin generates a signal by binding to a surface receptor or an associated transporter, triggering signaling cascades that activate *ciaRH* and the *comCDE* genes. The generated CSP-1 is exported and activated an unknown TCS that mediates biofilm formation.

Disclaimer: I, Fahmina Akhter, conceived and contributed to the design and implementation of the research for the two chapters presented in this dissertation. I received some strains as a generous gift from Dr. Jorge E Vidal that I used in some experiments in both chapter one and chapter two. With consultation with Dr. Zehava Eichenbaum, I wrote two manuscripts based on the findings in chapter one and chapter two. Other co-authors in the manuscripts contributed to some of the experiments. I conducted the RNA-Seq experiments with the help of Dr. Yoann Le Breton, and Dr. Kevin S. McIver using the sequencing facility at the University of Maryland, College Park. I performed the RNA-Seq data analyses with the help of Dr. Shrikant Pawar. Edroyal Womack contributed to some of the mutant construction and growth assay.

REFERENCES

1. Kadioglu, A., et al., *The role of Streptococcus pneumoniae virulence factors in host respiratory colonization and disease.* Nat Rev Microbiol, 2008. **6**(4): p. 288-301.
2. Adegbola, R.A., et al., *Carriage of Streptococcus pneumoniae and other respiratory bacterial pathogens in low and lower-middle income countries: a systematic review and meta-analysis.* PLoS One, 2014. **9**(8): p. e103293.
3. Chao, Y., et al., *Streptococcus pneumoniae biofilm formation and dispersion during colonization and disease.* Front Cell Infect Microbiol, 2014. **4**: p. 194.
4. Korona-Glowniak, I. and A. Malm, *Characteristics of Streptococcus pneumoniae strains colonizing upper respiratory tract of healthy preschool children in Poland.* ScientificWorldJournal, 2012. **2012**: p. 732901.
5. Klugman, K.P., S.A. Madhi, and W.C. Albrich, *Novel approaches to the identification of Streptococcus pneumoniae as the cause of community-acquired pneumonia.* Clin Infect Dis, 2008. **47 Suppl 3**: p. S202-6.
6. van der Poll, T. and S.M. Opal, *Pathogenesis, treatment, and prevention of pneumococcal pneumonia.* Lancet, 2009. **374**(9700): p. 1543-56.
7. Levine, O.S. and K.P. Klugman, *Editorial: Breathing new life into pneumonia epidemiology.* Am J Epidemiol, 2009. **170**(9): p. 1067-8.
8. Walker, C.L.F., et al., *Global burden of childhood pneumonia and diarrhoea.* Lancet, 2013. **381**(9875): p. 1405-1416.
9. Eurich, D.T., et al., *Risk of heart failure after community acquired pneumonia: prospective controlled study with 10 years of follow-up.* BMJ, 2017. **356**: p. j413.

10. Musher, D.M., et al., *The association between pneumococcal pneumonia and acute cardiac events.* Clin Infect Dis, 2007. **45**(2): p. 158-65.

11. Jedrzejas, M.J., *Pneumococcal virulence factors: structure and function.* Microbiol Mol Biol Rev, 2001. **65**(2): p. 187-207 ; first page, table of contents.

12. Davis, B.M., et al., *Influenza and community-acquired pneumonia interactions: the impact of order and time of infection on population patterns.* Am J Epidemiol, 2012. **175**(5): p. 363-7.

13. Klein, E.Y., et al., *The frequency of influenza and bacterial coinfection: a systematic review and meta-analysis.* Influenza Other Respir Viruses, 2016. **10**(5): p. 394-403.

14. *Estimates of the global, regional, and national morbidity, mortality, and aetiologies of lower respiratory infections in 195 countries, 1990-2016: a systematic analysis for the Global Burden of Disease Study 2016.* Lancet Infect Dis, 2018. **18**(11): p. 1191-1210.

15. Brooks, L.R.K. and G.I. Mias, *Streptococcus pneumoniae's Virulence and Host Immunity: Aging, Diagnostics, and Prevention.* Front Immunol, 2018. **9**: p. 1366.

16. Gamez, G., et al., *The variome of pneumococcal virulence factors and regulators.* BMC Genomics, 2018. **19**(1): p. 10.

17. Weiser, J.N., D.M. Ferreira, and J.C. Paton, *Streptococcus pneumoniae: transmission, colonization and invasion.* Nat Rev Microbiol, 2018. **16**(6): p. 355-367.

18. Philips, B.J., et al., *Factors determining the appearance of glucose in upper and lower respiratory tract secretions.* Intensive Care Med, 2003. **29**(12): p. 2204-2210.

19. Shelburne, S.A., et al., *The role of complex carbohydrate catabolism in the pathogenesis of invasive streptococci.* Trends Microbiol, 2008. **16**(7): p. 318-25.

20. Rose, M.C. and J.A. Voynow, *Respiratory tract mucin genes and mucin glycoproteins in health and disease.* Physiol Rev, 2006. **86**(1): p. 245-78.

21. Yesilkaya, H., et al., *The ability to utilize mucin affects the regulation of virulence gene expression in Streptococcus pneumoniae.* FEMS Microbiol Lett, 2008. **278**(2): p. 231-5.

22. Burnaugh, A.M., L.J. Frantz, and S.J. King, *Growth of Streptococcus pneumoniae on human glycoconjugates is dependent upon the sequential activity of bacterial exoglycosidases.* J Bacteriol, 2008. **190**(1): p. 221-30.

23. Terra, V.S., et al., *Characterization of novel beta-galactosidase activity that contributes to glycoprotein degradation and virulence in Streptococcus pneumoniae.* Infect Immun, 2010. **78**(1): p. 348-57.

24. Gosink, K.K., et al., *Role of novel choline binding proteins in virulence of Streptococcus pneumoniae.* Infect Immun, 2000. **68**(10): p. 5690-5.

25. Bergmann, S. and S. Hammerschmidt, *Versatility of pneumococcal surface proteins.* Microbiology, 2006. **152**(Pt 2): p. 295-303.

26. Hartel, T., et al., *Impact of glutamine transporters on pneumococcal fitness under infection-related conditions.* Infect Immun, 2011. **79**(1): p. 44-58.

27. JS, D.C.a.B., *Streptococcus pneumoniae lipoproteins and ABC transporters. In Streptococcus pneumoniae: Molecular Mechanisms of Host-Pathogen Interactions (Brown JS, Hammerschmidt S and Orihuela C, eds).* 2015: p. pp. 347–362.

28. Kerr, A.R., et al., *The Ami-AliA/AliB permease of Streptococcus pneumoniae is involved in nasopharyngeal colonization but not in invasive disease.* Infect Immun, 2004. **72**(7): p. 3902-6.

29. Kohler, S., et al., *Pneumococcal lipoproteins involved in bacterial fitness, virulence, and immune evasion.* FEBS Lett, 2016. **590**(21): p. 3820-3839.

30. Ogunniyi, A.D., et al., *Identification of genes that contribute to the pathogenesis of invasive pneumococcal disease by in vivo transcriptomic analysis.* Infect Immun, 2012. **80**(9): p. 3268-78.

31. Pribyl, T., et al., *Influence of impaired lipoprotein biogenesis on surface and exoproteome of Streptococcus pneumoniae.* J Proteome Res, 2014. **13**(2): p. 650-67.

32. Miethke, M., *Molecular strategies of microbial iron assimilation: from high-affinity complexes to cofactor assembly systems.* Metallomics, 2013. **5**(1): p. 15-28.

33. Skaar, E.P., *The battle for iron between bacterial pathogens and their vertebrate hosts.* PLoS Pathog, 2010. **6**(8): p. e1000949.

34. Bullen, J.J., et al., *Natural resistance, iron and infection: a challenge for clinical medicine.* J Med Microbiol, 2006. **55**(Pt 3): p. 251-258.

35. Tong, Y. and M. Guo, *Bacterial heme-transport proteins and their heme-coordination modes.* Arch Biochem Biophys, 2009. **481**(1): p. 1-15.

36. Chiabrando, D., et al., *Heme in pathophysiology: a matter of scavenging, metabolism and trafficking across cell membranes.* Front Pharmacol, 2014. **5**: p. 61.

37. Maines, M.D. and A. Kappas, *The degradative effects of porphyrins and heme compounds on components of the microsomal mixed function oxidase system.* J Biol Chem, 1975. **250**(6): p. 2363-9.

38. Solar, I., J. Dulitzky, and N. Shaklai, *Hemin-promoted peroxidation of red cell cytoskeletal proteins.* Arch Biochem Biophys, 1990. **283**(1): p. 81-9.

39. Brown, J.S. and D.W. Holden, *Iron acquisition by Gram-positive bacterial pathogens.* Microbes Infect, 2002. **4**(11): p. 1149-56.

40. Nobles, C.L. and A.W. Maresso, *The theft of host heme by Gram-positive pathogenic bacteria.* Metallomics, 2011. **3**(8): p. 788-96.

41. Johnson, E.E. and M. Wessling-Resnick, *Iron metabolism and the innate immune response to infection.* Microbes Infect, 2012. **14**(3): p. 207-16.

42. Beutler, E. and J. Waalen, *The definition of anemia: what is the lower limit of normal of the blood hemoglobin concentration?* Blood, 2006. **107**(5): p. 1747-50.

43. Tai, S.S., C.J. Lee, and R.E. Winter, *Hemin utilization is related to virulence of Streptococcus pneumoniae.* Infect Immun, 1993. **61**(12): p. 5401-5.

44. Brown, J.S., S.M. Gilliland, and D.W. Holden, *A Streptococcus pneumoniae pathogenicity island encoding an ABC transporter involved in iron uptake and virulence.* Mol Microbiol, 2001. **40**(3): p. 572-85.

45. Brown, J.S., et al., *Characterization of pit, a Streptococcus pneumoniae iron uptake ABC transporter.* Infect Immun, 2002. **70**(8): p. 4389-98.

46. Cao, K., et al., *Evolution and molecular mechanism of PitAs in iron transport of Streptococcus species.* J Inorg Biochem, 2018. **182**: p. 113-123.

47. Tai, S.S., C. Yu, and J.K. Lee, *A solute binding protein of Streptococcus pneumoniae iron transport.* FEMS Microbiol Lett, 2003. **220**(2): p. 303-8.

48. Cheng, W., et al., *Structures of Streptococcus pneumoniae PiaA and its complex with ferrichrome reveal insights into the substrate binding and release of high affinity iron transporters.* PLoS One, 2013. **8**(8): p. e71451.

49. Tettelin, H., et al., *Complete genome sequence of a virulent isolate of Streptococcus pneumoniae.* Science, 2001. **293**(5529): p. 498-506.

50. Yang, X.Y., et al., *Integrated Translatomics with Proteomics to Identify Novel Iron-Transporting Proteins in Streptococcus pneumoniae.* Front Microbiol, 2016. **7**: p. 78.

51. Yang, X.Y., et al., *Lipoprotein SPD_1609 of Streptococcus pneumoniae Promotes Adherence and Invasion to Epithelial Cells Contributing to Bacterial Virulence.* Front Microbiol, 2019. **10**: p. 1769.

52. Romero-Espejel, M.E., et al., *Characterization of Spbhp-37, a Hemoglobin-Binding Protein of Streptococcus pneumoniae.* Front Cell Infect Microbiol, 2016. **6**: p. 47.

53. Miao, X., et al., *A Novel Iron Transporter SPD_1590 in Streptococcus pneumoniae Contributing to Bacterial Virulence Properties.* Front Microbiol, 2018. **9**: p. 1624.

54. Domenech, M., E. Garcia, and M. Moscoso, *Biofilm formation in Streptococcus pneumoniae.* Microb Biotechnol, 2012. **5**(4): p. 455-65.

55. Hall-Stoodley, L., et al., *Direct detection of bacterial biofilms on the middle-ear mucosa of children with chronic otitis media.* Jama, 2006. **296**(2): p. 202-11.

56. Sanderson, A.R., J.G. Leid, and D. Hunsaker, *Bacterial biofilms on the sinus mucosa of human subjects with chronic rhinosinusitis.* Laryngoscope, 2006. **116**(7): p. 1121-6.

57. Shenoy, A.T., et al., *Streptococcus pneumoniae in the heart subvert the host response through biofilm-mediated resident macrophage killing.* PLoS Pathog, 2017. **13**(8): p. e1006582.

58. Shak, J.R., J.E. Vidal, and K.P. Klugman, *Influence of bacterial interactions on pneumococcal colonization of the nasopharynx.* Trends Microbiol, 2013. **21**(3): p. 129-35.

59. Lattar, S.M., et al., *A Mechanism of Unidirectional Transformation, Leading to Antibiotic Resistance, Occurs within Nasopharyngeal Pneumococcal Biofilm Consortia.* MBio, 2018. **9**(3).

60. Pettigrew, M.M., et al., *Dynamic changes in the Streptococcus pneumoniae transcriptome during transition from biofilm formation to invasive disease upon influenza A virus infection.* Infect Immun, 2014. **82**(11): p. 4607-19.

61. Trappetti, C., et al., *Sialic acid: a preventable signal for pneumococcal biofilm formation, colonization, and invasion of the host.* J Infect Dis, 2009. **199**(10): p. 1497-505.

62. Blanchette, K.A., et al., *Neuraminidase A-Exposed Galactose Promotes Streptococcus pneumoniae Biofilm Formation during Colonization.* Infect Immun, 2016. **84**(10): p. 2922-32.

63. Rose, L., et al., *Antibodies against PsrP, a novel Streptococcus pneumoniae adhesin, block adhesion and protect mice against pneumococcal challenge.* J Infect Dis, 2008. **198**(3): p. 375-83.

64. Sanchez, C.J., et al., *The pneumococcal serine-rich repeat protein is an intra-species bacterial adhesin that promotes bacterial aggregation in vivo and in biofilms.* PLoS Pathog, 2010. **6**(8): p. e1001044.

65. Carvalho, S.M., O.P. Kuipers, and A.R. Neves, *Environmental and nutritional factors that affect growth and metabolism of the pneumococcal serotype 2 strain D39 and its nonencapsulated derivative strain R6.* PLoS One, 2013. **8**(3): p. e58492.

66. Goncalves, V.M., et al., *Purification of capsular polysaccharide from Streptococcus pneumoniae serotype 23F by a procedure suitable for scale-up.* Biotechnol Appl Biochem, 2003. **37**(Pt 3): p. 283-7.

67. Massaldi, H., et al., *Features of bacterial growth and polysaccharide production of Streptococcus pneumoniae serotype 14.* Biotechnol Appl Biochem, 2010. **55**(1): p. 37-43.

68. Slotved, H.C. and C. Satzke, *In vitro growth of pneumococcal isolates representing 23 different serotypes.* BMC Res Notes, 2013. **6**: p. 208.

69. Berry, A.M., et al., *Contribution of autolysin to virulence of Streptococcus pneumoniae.* Infect Immun, 1989. **57**(8): p. 2324-30.

70. Berry, A.M. and J.C. Paton, *Additive attenuation of virulence of Streptococcus pneumoniae by mutation of the genes encoding pneumolysin and other putative pneumococcal virulence proteins.* Infect Immun, 2000. **68**(1): p. 133-40.

71. Regev-Yochay, G., et al., *SpxB is a suicide gene of Streptococcus pneumoniae and confers a selective advantage in an in vivo competitive colonization model.* J Bacteriol, 2007. **189**(18): p. 6532-9.

72. Grousd, J.A., H.E. Rich, and J.F. Alcorn, *Host-Pathogen Interactions in Gram-Positive Bacterial Pneumonia.* Clin Microbiol Rev, 2019. **32**(3).

73. Lopez, C.A. and E.P. Skaar, *The Impact of Dietary Transition Metals on Host-Bacterial Interactions.* Cell Host Microbe, 2018. **23**(6): p. 737-748.

74. Palmer, L.D. and E.P. Skaar, *Transition Metals and Virulence in Bacteria.* Annu Rev Genet, 2016. **50**: p. 67-91.

75. Turner, A.G., et al., *Transition Metal Homeostasis in Streptococcus pyogenes and Streptococcus pneumoniae.* Adv Microb Physiol, 2017. **70**: p. 123-191.

76. Ge, R. and X. Sun, *Iron acquisition and regulation systems in Streptococcus species.* Metallomics, 2014. **6**(5): p. 996-1003.

77. O'Brien, K.L., et al., *Evaluation of a medium (STGG) for transport and optimal recovery of Streptococcus pneumoniae from nasopharyngeal secretions collected during field studies.* J Clin Microbiol, 2001. **39**(3): p. 1021-4.

78. Porter, R.D. and W.R. Guild, *Characterization of some pneumococcal bacteriophages.* J Virol, 1976. **19**(2): p. 659-67.

79. EPA, U.S., *Method 200.8: Determination of Trace Elements in Waters and Wastes by Inductively Coupled Plasma-Mass Spectrometry*. 1994.

80. EPA, U.S., *Method 3052: Microwave Assisted Acid Digestion of Siliceous and Organically Based Matrices.* 1996. **Revision 0**.

81. Vidal, J.E., et al., *The LuxS-dependent quorum-sensing system regulates early biofilm formation by Streptococcus pneumoniae strain D39.* Infect Immun, 2011. **79**(10): p. 4050-60.

82. Havarstein, L.S., G. Coomaraswamy, and D.A. Morrison, *An unmodified heptadecapeptide pheromone induces competence for genetic transformation in Streptococcus pneumoniae.* Proc Natl Acad Sci U S A, 1995. **92**(24): p. 11140-4.

83. Langmead, B., et al., *Ultrafast and memory-efficient alignment of short DNA sequences to the human genome.* Genome Biol, 2009. **10**(3): p. R25.

84. Liao, Y., G.K. Smyth, and W. Shi, *featureCounts: an efficient general purpose program for assigning sequence reads to genomic features.* Bioinformatics, 2014. **30**(7): p. 923-30.

85. Love, M.I., W. Huber, and S. Anders, *Moderated estimation of fold change and dispersion for RNA-seq data with DESeq2.* Genome Biol, 2014. **15**(12): p. 550.

86. Cook, L.C.C., et al., *Transcriptomic Analysis of Streptococcus pyogenes Colonizing the Vaginal Mucosa Identifies hupY, an MtsR-Regulated Adhesin Involved in Heme Utilization.* mBio, 2019. **10**(3).

87. Ponka, P., et al., *The effect of various chelating agents on the mobilization of iron from reticulocytes in the presence and absence of pyridoxal isonicotinoyl hydrazone.* Biochim Biophys Acta, 1984. **802**(3): p. 477-89.

88. King, K.Y., J.A. Horenstein, and M.G. Caparon, *Aerotolerance and peroxide resistance in peroxidase and PerR mutants of Streptococcus pyogenes.* J Bacteriol, 2000. **182**(19): p. 5290-9.

89. Bates, C.S., et al., *Identification and characterization of a Streptococcus pyogenes operon involved in binding of hemoproteins and acquisition of iron.* Infect Immun, 2003. **71**(3): p. 1042-55.

90. Bai, X.H., et al., *Structure of pneumococcal peptidoglycan hydrolase LytB reveals insights into the bacterial cell wall remodeling and pathogenesis.* J Biol Chem, 2014. **289**(34): p. 23403-16.

91. Eijkelkamp, B.A., et al., *The First Histidine Triad Motif of PhtD Is Critical for Zinc Homeostasis in Streptococcus pneumoniae.* Infect Immun, 2016. **84**(2): p. 407-15.

92. Jensch, I., et al., *PavB is a surface-exposed adhesin of Streptococcus pneumoniae contributing to nasopharyngeal colonization and airways infections.* Mol Microbiol, 2010. **77**(1): p. 22-43.

93. Romero-Espejel, M.E., M.A. Gonzalez-Lopez, and J. Olivares-Trejo Jde, *Streptococcus pneumoniae requires iron for its viability and expresses two membrane proteins that bind haemoglobin and haem.* Metallomics, 2013. **5**(4): p. 384-9.

94. Shafeeq, S., O.P. Kuipers, and T.G. Kloosterman, *Cellobiose-mediated gene expression in Streptococcus pneumoniae: a repressor function of the novel GntR-type regulator BguR.* PLoS One, 2013. **8**(2): p. e57586.

95. Bidossi, A., et al., *A functional genomics approach to establish the complement of carbohydrate transporters in Streptococcus pneumoniae.* PLoS One, 2012. **7**(3): p. e33320.

96. Dehal, P.S., et al., *MicrobesOnline: an integrated portal for comparative and functional genomics.* Nucleic Acids Res, 2010. **38**(Database issue): p. D396-400.

97. Anzaldi, L.L. and E.P. Skaar, *Overcoming the heme paradox: heme toxicity and tolerance in bacterial pathogens.* Infect Immun, 2010. **78**(12): p. 4977-89.

98. Sachla, A.J., et al., *The crimson conundrum: heme toxicity and tolerance in GAS.* Front Cell Infect Microbiol, 2014. **4**: p. 159.

99. Sheldon, J.R. and D.E. Heinrichs, *Recent developments in understanding the iron acquisition strategies of gram positive pathogens.* FEMS Microbiol Rev, 2015. **39**(4): p. 592-630.

100. Montanez, G.E., M.N. Neely, and Z. Eichenbaum, *The streptococcal iron uptake (Siu) transporter is required for iron uptake and virulence in a zebrafish infection model.* Microbiology, 2005. **151**(Pt 11): p. 3749-3757.

101. Rouault, T.A., *Microbiology. Pathogenic bacteria prefer heme.* Science, 2004. **305**(5690): p. 1577-8.

102. Lyles, K.V. and Z. Eichenbaum, *From Host Heme To Iron: The Expanding Spectrum of Heme Degrading Enzymes Used by Pathogenic Bacteria.* Front Cell Infect Microbiol, 2018. **8**: p. 198.

103. Foresti, R., C.J. Green, and R. Motterlini, *Generation of bile pigments by haem oxygenase: a refined cellular strategy in response to stressful insults.* Biochem Soc Symp, 2004(71): p. 177-92.

104. Vitek, L. and H.A. Schwertner, *The heme catabolic pathway and its protective effects on oxidative stress-mediated diseases.* Adv Clin Chem, 2007. **43**: p. 1-57.

105. Mercade, M., N.D. Lindley, and P. Loubiere, *Metabolism of Lactococcus lactis subsp. cremoris MG 1363 in acid stress conditions.* Int J Food Microbiol, 2000. **55**(1-3): p. 161-5.

106. Claverys, J.P., B. Grossiord, and G. Alloing, *Is the Ami-AliA/B oligopeptide permease of Streptococcus pneumoniae involved in sensing environmental conditions?* Res Microbiol, 2000. **151**(6): p. 457-63.

107. Cundell, D.R., et al., *Peptide permeases from Streptococcus pneumoniae affect adherence to eucaryotic cells.* Infect Immun, 1995. **63**(7): p. 2493-8.

108. Piet, J.R., et al., *Streptococcus pneumoniae arginine synthesis genes promote growth and virulence in pneumococcal meningitis.* J Infect Dis, 2014. **209**(11): p. 1781-91.

109. Paixao, L., et al., *Host glycan sugar-specific pathways in Streptococcus pneumoniae: galactose as a key sugar in colonisation and infection [corrected]*. PLoS One, 2015. **10**(3): p. e0121042.

110. Minhas, V., et al., *Capacity To Utilize Raffinose Dictates Pneumococcal Disease Phenotype.* MBio, 2019. **10**(1).

111. *CDC. Antibiotic Resistance Threats in the United States, 2019. Atlanta, GA: U.S. Department of Health and Human Services, CDC; 2019.* 2019.

112. Avery, O.T., C.M. Macleod, and M. McCarty, *Studies on the Chemical Nature of the Substance Inducing Transformation of Pneumococcal Types : Induction of Transformation by a Desoxyribonucleic Acid Fraction Isolated from Pneumococcus Type Iii.* J Exp Med, 1944. **79**(2): p. 137-58.

113. Lanie, J.A., et al., *Genome sequence of Avery's virulent serotype 2 strain D39 of Streptococcus pneumoniae and comparison with that of unencapsulated laboratory strain R6.* J Bacteriol, 2007. **189**(1): p. 38-51.

114. Chenoweth, C.E., et al., *Antimicrobial resistance in Streptococcus pneumoniae: implications for patients with community-acquired pneumonia.* Mayo Clin Proc, 2000. **75**(11): p. 1161-8.

115. Kim, L., et al., *Biological and Epidemiological Features of Antibiotic-Resistant Streptococcus pneumoniae in Pre- and Post-Conjugate Vaccine Eras: a United States Perspective.* Clin Microbiol Rev, 2016. **29**(3): p. 525-52.

116. Budhani, R.K. and J.K. Struthers, *The use of Sorbarod biofilms to study the antimicrobial susceptibility of a strain of Streptococcus pneumoniae.* J Antimicrob Chemother, 1997. **40**(4): p. 601-2.

117. Donlan, R.M., et al., *Model system for growing and quantifying Streptococcus pneumoniae biofilms in situ and in real time.* Appl Environ Microbiol, 2004. **70**(8): p. 4980-8.

118. Marks, L.R., G.I. Parameswaran, and A.P. Hakansson, *Pneumococcal interactions with epithelial cells are crucial for optimal biofilm formation and colonization in vitro and in vivo.* Infect Immun, 2012. **80**(8): p. 2744-60.

119. Parker, D., et al., *The NanA neuraminidase of Streptococcus pneumoniae is involved in biofilm formation.* Infect Immun, 2009. **77**(9): p. 3722-30.

120. Vidal, J.E., et al., *Quorum-sensing systems LuxS/autoinducer 2 and Com regulate Streptococcus pneumoniae biofilms in a bioreactor with living cultures of human respiratory cells.* Infect Immun, 2013. **81**(4): p. 1341-53.

121. Trappetti, C., et al., *Extracellular matrix formation enhances the ability of Streptococcus pneumoniae to cause invasive disease.* PLoS One, 2011. **6**(5): p. e19844.

122. Weimer, K.E., et al., *Coinfection with Haemophilus influenzae promotes pneumococcal biofilm formation during experimental otitis media and impedes the progression of pneumococcal disease.* J Infect Dis, 2010. **202**(7): p. 1068-75.

123. Moscoso, M., E. Garcia, and R. Lopez, *Biofilm formation by Streptococcus pneumoniae: role of choline, extracellular DNA, and capsular polysaccharide in microbial accretion.* J Bacteriol, 2006. **188**(22): p. 7785-95.

124. Oggioni, M.R., et al., *Switch from planktonic to sessile life: a major event in pneumococcal pathogenesis.* Mol Microbiol, 2006. **61**(5): p. 1196-210.

125. Munoz-Elias, E.J., J. Marcano, and A. Camilli, *Isolation of Streptococcus pneumoniae biofilm mutants and their characterization during nasopharyngeal colonization.* Infect Immun, 2008. **76**(11): p. 5049-61.

126. Blanchette-Cain, K., et al., *Streptococcus pneumoniae biofilm formation is strain dependent, multifactorial, and associated with reduced invasiveness and immunoreactivity during colonization.* MBio, 2013. **4**(5): p. e00745-13.

127. Mayanskiy, A.N., et al., *[BIOFILM FORMATION BY STREPTOCOCCUS PNEUMONIAE].* Mol Gen Mikrobiol Virusol, 2015. **33**(3): p. 16-22.

128. Trappetti, C., et al., *The impact of the competence quorum sensing system on Streptococcus pneumoniae biofilms varies depending on the experimental model.* BMC Microbiol, 2011. **11**: p. 75.

129. Berry, A.M., et al., *Effect of defined point mutations in the pneumolysin gene on the virulence of Streptococcus pneumoniae.* Infect Immun, 1995. **63**(5): p. 1969-74.

130. Bokori-Brown, M., et al., *Red Blood Cell Susceptibility to Pneumolysin: CORRELATION WITH MEMBRANE BIOCHEMICAL AND PHYSICAL PROPERTIES.* J Biol Chem, 2016. **291**(19): p. 10210-27.

131. Shewell, L.K., et al., *The cholesterol-dependent cytolysins pneumolysin and streptolysin O require binding to red blood cell glycans for hemolytic activity.* Proc Natl Acad Sci U S A, 2014. **111**(49): p. E5312-20.

132. Allan, R.N., et al., *Pronounced metabolic changes in adaptation to biofilm growth by Streptococcus pneumoniae.* PLoS One, 2014. **9**(9): p. e107015.

133. Embry, A., E. Hinojosa, and C.J. Orihuela, *Regions of Diversity 8, 9 and 13 contribute to Streptococcus pneumoniae virulence.* BMC Microbiol, 2007. **7**: p. 80.

134. Hoover, S.E., et al., *A new quorum-sensing system (TprA/PhrA) for Streptococcus pneumoniae D39 that regulates a lantibiotic biosynthesis gene cluster.* Mol Microbiol, 2015. **97**(2): p. 229-43.

135. Sanchez, C.J., et al., *Streptococcus pneumoniae in biofilms are unable to cause invasive disease due to altered virulence determinant production.* PLoS One, 2011. **6**(12): p. e28738.

136. Trappetti, C., et al., *LuxS mediates iron-dependent biofilm formation, competence, and fratricide in Streptococcus pneumoniae.* Infect Immun, 2011. **79**(11): p. 4550-8.

137. Bortoni, M.E., et al., *The pneumococcal response to oxidative stress includes a role for Rgg.* Microbiology, 2009. **155**(Pt 12): p. 4123-4134.

138. Karlsson, D., et al., *Modeling the regulation of the competence-evoking quorum sensing network in Streptococcus pneumoniae.* Biosystems, 2007. **90**(1): p. 211-23.

139. Prudhomme, M., et al., *Pneumococcal Competence Coordination Relies on a Cell-Contact Sensing Mechanism.* PLoS Genet, 2016. **12**(6): p. e1006113.

140. Dawid, S., M.E. Sebert, and J.N. Weiser, *Bacteriocin activity of Streptococcus pneumoniae is controlled by the serine protease HtrA via posttranscriptional regulation.* J Bacteriol, 2009. **191**(5): p. 1509-18.

141. Halfmann, A., et al., *Activity of the two-component regulatory system CiaRH in Streptococcus pneumoniae R6.* J Mol Microbiol Biotechnol, 2011. **20**(2): p. 96-104.

142. Mascher, T., et al., *The CiaRH system of Streptococcus pneumoniae prevents lysis during stress induced by treatment with cell wall inhibitors and by mutations in pbp2x involved in beta-lactam resistance.* J Bacteriol, 2006. **188**(5): p. 1959-68.

143. Sebert, M.E., et al., *Microarray-based identification of htrA, a Streptococcus pneumoniae gene that is regulated by the CiaRH two-component system and contributes to nasopharyngeal colonization.* Infect Immun, 2002. **70**(8): p. 4059-67.

144. Hentrich, K., et al., *Streptococcus pneumoniae Senses a Human-like Sialic Acid Profile via the Response Regulator CiaR.* Cell Host Microbe, 2016. **20**(3): p. 307-317.

145. King, S.J., K.R. Hippe, and J.N. Weiser, *Deglycosylation of human glycoconjugates by the sequential activities of exoglycosidases expressed by Streptococcus pneumoniae.* Mol Microbiol, 2006. **59**(3): p. 961-74.

146. Cvitkovitch, D.G., Y.H. Li, and R.P. Ellen, *Quorum sensing and biofilm formation in Streptococcal infections.* J Clin Invest, 2003. **112**(11): p. 1626-32.

147. Li, Y.H., et al., *A quorum-sensing signaling system essential for genetic competence in Streptococcus mutans is involved in biofilm formation.* J Bacteriol, 2002. **184**(10): p. 2699-708.

148. Rodriguez, A.M., et al., *Physiological and molecular characterization of genetic competence in Streptococcus sanguinis.* Mol Oral Microbiol, 2011. **26**(2): p. 99-116.

149. Zhu, B., et al., *A Novel Regulator Modulates Glucan Production, Cell Aggregation and Biofilm Formation in Streptococcus sanguinis SK36.* Front Microbiol, 2018. **9**: p. 1154.

150. Pynnonen, M., et al., *Hemoglobin promotes Staphylococcus aureus nasal colonization.* PLoS Pathog, 2011. **7**(7): p. e1002104.

151. Shak, J.R., et al., *Novel role for the Streptococcus pneumoniae toxin pneumolysin in the assembly of biofilms.* MBio, 2013. **4**(5): p. e00655-13.

152. Nieto, C. and M. Espinosa, *Construction of the mobilizable plasmid pMV158GFP, a derivative of pMV158 that carries the gene encoding the green fluorescent protein.* Plasmid, 2003. **49**(3): p. 281-5.

153. Allegrucci, M., et al., *Phenotypic characterization of Streptococcus pneumoniae biofilm development.* J Bacteriol, 2006. **188**(7): p. 2325-35.

APPENDICES

Appendix A: Correlation of gene expression by RNA-seq and qRT-PCR

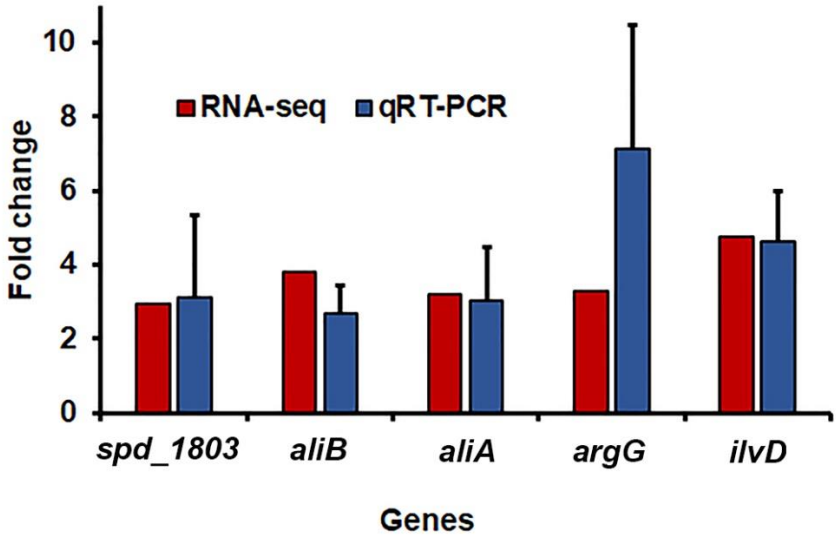

RNA extracted from cell 1hr post hemoglobin treatment was used to measure the gene expression by qRT-PCR. The relative expression was calculated using ΔΔCt method with the comparison of +/- hemoglobin treated samples and normalized to *gyrB* gene in which the expression was not changed in the RNA-Seq analysis. The experiments were performed in duplicates with three biological replicates. The replicates data are shown as the mean ± SD.